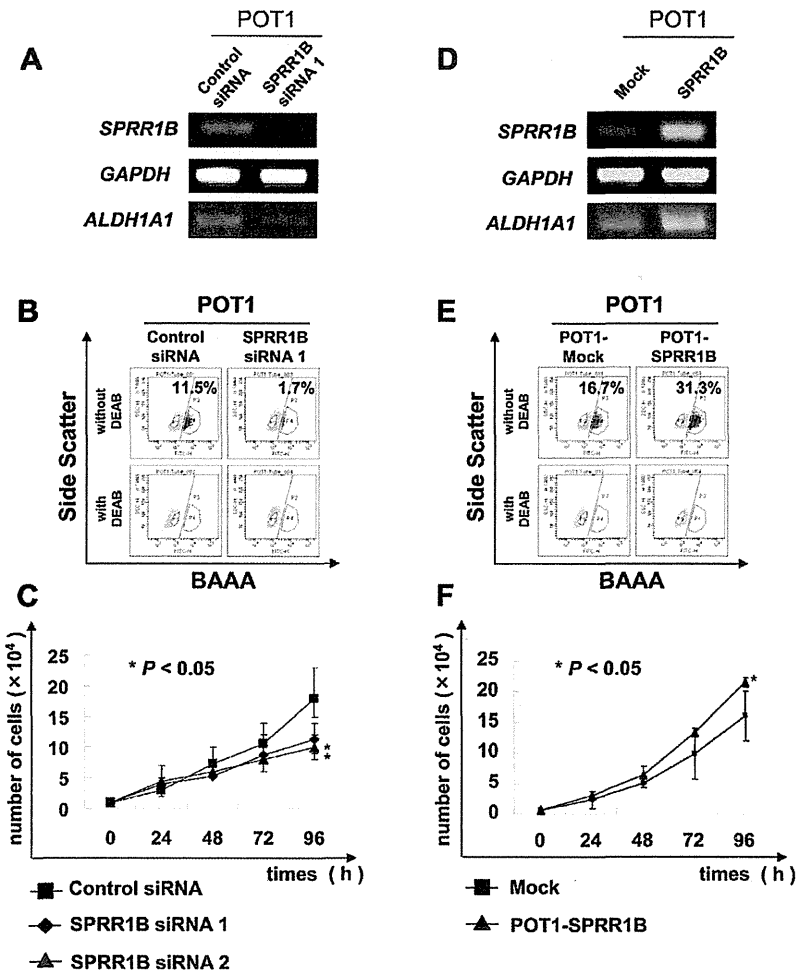

Fig. 3. SPRR1B has a role in cell growth of OSCC. (A) RT-PCR of SPRR1B knockdown cells. *SPRR1B* siRNA was transfected into POT1 cells. Twenty-four hours after transfection, total RNAs were purified and the expression of SPRR1B and ALDH1A1 was evaluated by RT-PCR. *GAPDH* was used as an internal control. (B) ALDEFLUOR assay. *SPRR1B* knockdown cells were analyzed by the ALDEFLUOR assay. Percentage represents the proportion of ALDH1^{br} cells. (C) *In vitro* cell growth. *In vitro* growth of *SPRR1B* siRNA-transfected POT1 cells were evaluated by cell count. Differences between control siRNA-transfected POT1 cells and *SPRR1B* siRNA-transfected POT1 cells were examined for statistical significance using Student's *t*-test. *$P < 0.05$. (D) RT-PCR of SPRR1B-overexpressed cells. Cells stably transfected with SPRR1B and control vector-transfected cells were used. The expression of SPRR1B and ALDH1A1 was evaluated by RT-PCR. *GAPDH* was used as an internal control. (E) ALDEFLUOR assay. *SPRR1B*-overexpressed cells were analyzed by the ALDEFLUOR assay. Percentage represents the proportion of ALDH1^{br} cells. (F) *In vitro* cell growth. *In vitro* growth of *SPRR1B*-overexpressed POT1 cells was evaluated by cell count. Differences between control vector-transfected POT1 cells and *SPRR1B*-transfected POT1 cells were examined for statistical significance using Student's *t*-test. *$P < 0.05$.

2.9. Statistical analysis

In the xenograft model and *in vitro* cell growth data, samples were analyzed using Student's *t*-test, with $P < 0.05$ conferring statistical significance.

3. Results

3.1. Isolation of OSCC stem-like cells

We used the ALDEFLUOR assay to isolate CSCs/CICs from OSCC cell lines. An ALDEFLUOR bright (ALDH1^{br}) population was detected in all of the cell lines (Fig. 1A and B). The proportions of ALDH1^{br} cells ranged from 12.2% for OSC20 to 28.4% for OSC19. To confirm that CSCs/CICs were enriched in ALDH1^{br} cells, we performed RT-PCR, sphere formation and tumor formation *in vivo* using NOD/SCID mice. We examined the expression of stem/progenitor cell genes including, *SOX2*, *POU5F1* and *NANOG* [21–24]. The ALDH1^{br} population expressed *ALDH1A1*, *SOX2*, *POU5F1* and *NANOG* at higher levels than those in the ALDH1^{low} population (Fig. 1C). Spheroid-like bodies were observed in POT1 ALDH1^{br} cells under the condition of culture in DMEM/F12 serum-free medium containing bFGF and EGF, whereas spheroid-like bodies were not observed in POT1 ALDH1^{low} cells (Fig. 1D).

To evaluate the *in vivo* tumor-initiating ability of ALDH1^{br} and ALDH1^{low} cells, we injected 10^2, 10^3, 10^4 and 10^5 cells into the backs of NOD/SCID mice. Tumor growth was initiated in 80% (4/5) and 100% (5/5) of the 10^3 and 10^4 ALDH1^{br}-injected mice, respectively (Table 1). On the other hand, tumor growth was initiated in 40% (2/5) and 60% (3/5) of the 10^3 and 10^4 ALDH1^{low}-injected mice, respectively. The tumors derived from 10^3 and 10^4 of ALDH1^{br} cells grew faster than those derived from ALDH1^{low} cells (Fig. 1E). The histologic findings showed no differences (Fig. 1F). These results indicate that CSCs/CICs were enriched in POT1 ALDH1^{br} cells.

3.2. Isolation of an OSCC stem-like cell-specific gene, SPRR1B

To analyze the molecular mechanisms of ALDH1^{br} cells, we screened for ALDH1^{br} cell-specific genes using a micro-array. The

overexpressed genes (rate > 2.0) in POT1 ALDH1^{br} cells are summarized in Table S2. To isolate a common OSCC CSC/CIC gene, we screened for an ALDH1^{br}-specific gene by RT-PCR using cDNAs derived from OSC70 ALDH1^{br} cells and ALDH1^{low} cells (Fig. S1). *Small proline-rich protein-1B (SPRR1B)* showed ALDH1^{br} cell-specific expression, and we therefore extended the RT-PCR study to other OSCC cells. *SPRR1B* showed ALDH1^{br} cell-specific expression in all cell lines (Fig. 2A). *SPRR1B* was expressed in esophagus, tongue and skin, which contain squamous cell epithelia, but was not expressed in other organs including the heart, brain, placenta, lung, liver, kidney, skeletal muscle, pancreas, spleen, thymus, prostate, testis, ovary, small intestine, colon, leukocytes and skin (Fig. 2B).

3.3. Regulation of ALDH^{br} cell growth by SPRR1B

To further investigate the role of *SPRR1B*, SPRR1B knockdown and overexpression experiments were performed. Three SPRR1B gene-specific siRNAs were confirmed for suppression of SPRR1B mRNA by RT-PCR. *SPRR1B* gene knockdown reduced the expression of *ALDH1* compared to that in control siRNA-transfected POT1 cells (Fig. 3A). *SPRR1B* gene knockdown reduced the ALDH1^{br} population compared to that in control siRNA-transfected POT1 cells (11.5–1.7%) (Fig. 3B). SPRR1B gene knockdown suppressed POT1 cell growth significantly compared with the growth of control siRNA-transfected POT1 cells (Fig. 3C).

On the other hand, the expression of ALDH1 was enhanced in SPRR1B-overexpressed POT1 cells compared with the expression in control vector-transfected POT1 cells (Fig. 3D). The proportion of ALDH1^{br} cells and cell growth rate were enhanced in SPRR1B-overexpressed POT1 cells compared with those in control vector-transfected POT1 cells (Fig. 3E and F).

3.4. Role of SPRR1B in cell grow by suppression of the tumor suppressor RASSF4

To search for a downstream gene of SPRR1B, we performed further microarray screening. *RASSF4* and *STEAP1* genes were downregulated in SPRR1B-overexpressed cells and *RASSF4* and *STEAP1* genes were upregulated in SPRR1B knockdown cells (Fig. S2). Ras association domain family member 4 (*RASSF4*) contains an RA (Ras association) domain and works as a Ras effector and it has role as a tumor suppressor gene. We therefore hypothesized that

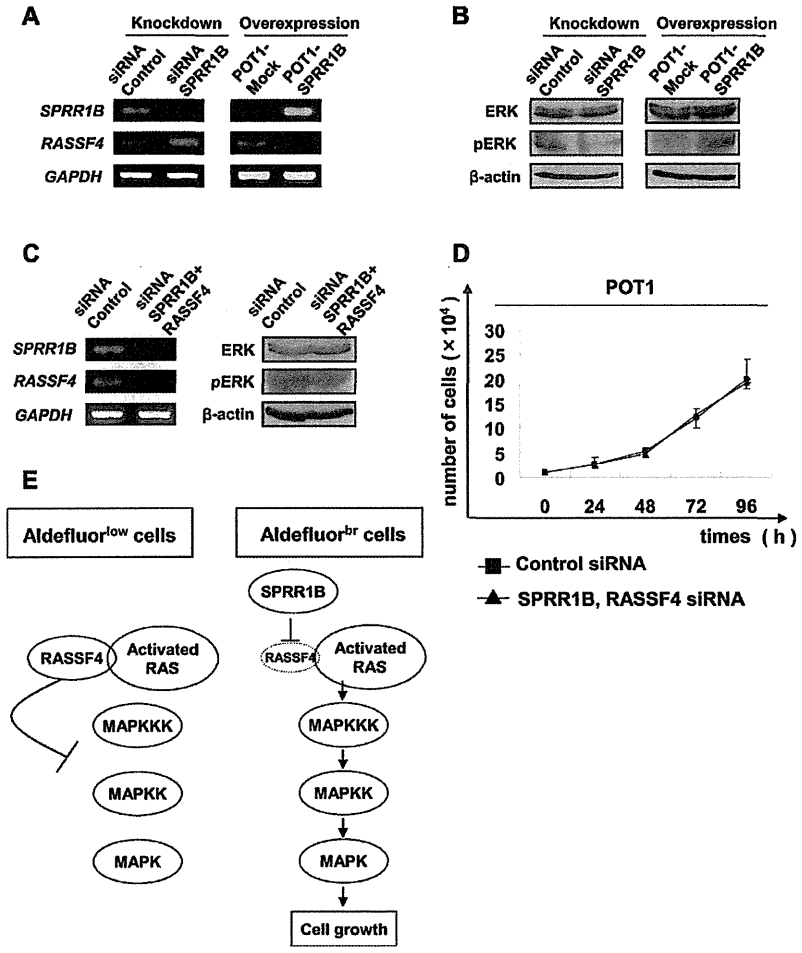

Fig. 4. *RASSF4* is negatively regulated by SPRR1B and has a role in inhibition of MAP kinase signal and cell growth. (A) RT-PCR of SPRR1B knockdown cells and SPRR1B-overexpressed cells. SPRR1B knockdown cells and SPRR1B-overexpressed cells were analyzed by RT-PCR. The expression of *SPRR1B* and *RASSF4* was evaluated. *GAPDH* was used as an internal control. (B) Western blot of MAP kinase signals using *SPRR1B* knockdown cells and SPRR1B-overexpressed cells. Total ERK protein and the phosphorylated form of ERK protein were detected by Western blotting. β-Actin was used as an internal control. (C) RT-PCR and Western blot analysis of SPRR1B and RASSF4 siRNA-transfected cells. Control siRNA or SPRR1B and RASSF4 siRNA was transfected into POT1 cells. The expression of SPRR1B and RASSF4 was evaluated by RT-PCR. Phosphorylation of ERK was evaluated by Western blot analysis. (D) *In vitro* growth of SPRR1B siRNA- and RASS4 siRNA-transfected POT1 cells. Data represent means ± SD. (E) Schematic model of SPRR1B related to growth of ALDH1^{br} cells.

downregulation of the *RASSF4* gene is one of the mechanisms of the enhancement of cell grow by SPRR1B overexpression.

To confirm the gene expression regulation, RT-PCR was performed. Expression of *RASSF4* was upregulated in SPRR1B siRNA-transfected cells compared with that in of control siRNA-transfected cells. On the other hand, expression of RASSF4 was downregulated in SPRR1B-overexpressed cells (Fig. 4A). Since RASSF4 has an RA domain and has a role as a tumor suppressor, we hypothesized that RASSF4 suppresses the MAP kinase signal, which is one of the major cell growth signals. The phosphorylated form of ERK was downregulated by transfection of SPRR1B siRNA compared with that in control siRNA-transfected cells. On the other hand, the phosphorylated form of ERK was upregulated by overexpression of SPRR1B compared with that in control vector-transfected cells (Fig. 4B).

To verify that the ERK inhibition effect is due to RASSF4, we transfected RASSF4-specific siRNA into SPRR1B siRNA-transfected cells. The amount of the phosphorylated form of ERK was the same as that in control siRNA-transfected cells (Fig. 4C). The growth rates of SPRR1B siRNA- and RASSF4 siRNA-transfected cells were same as the growth rate of control siRNA-transfected cells (Fig. 4D).

4. Discussion

In this study, we isolated oral CSCs/CICs as ALDH1^{br} cells. The tumor-initiating ability of ALDH1^{br} cells were confirmed by using NOD/SCID mice that ALDH1^{br} cells derived from POT1 cells showed higher tumor initiation ability than that of ALDH1^{low} cells. Furthermore, ALDH1^{br} cells more efficiently produced tumor spheres than did ALDH1^{low} cells and showed higher levels of stem cell markers including *SOX2*, *POU5F1* and *NANOG*; thus, POT1 ALDH1^{br} cells are likely to be enriched with a CSC/CIC population and should be suitable for analysis of OSCC CSCs/CICs.

The *SPRR* gene family includes 17 genes comprising four subfamilies [25,26]. SPRRs are structural proteins and they form a cornified cell envelop (CE) with other structural proteins such as involucrin and loricrin and are thought to work as a barrier [27]. SPRRs, especially SPRR3, have been reported to be up-regulated in malignant diseases [28,29]. Cho et al. reported that SPRR3 activated AKT and decreased the expression of p53 through the activation of MDM2 in colon cancer cells. On the other hand, overexpression of SPRR1B was reported to induce G0 cell cycle arrest in Chinese hamster ovary (CHO) cells [30]. In this study, overexpression of the *SPRR1B* gene enhanced cell grow *in vitro* and increased the ALDH1^{br} population in POT1 cells. Thus, the *SPRR1B* gene has a role to enhance cell growth of OSCC but not in CHO cells. One of the mechanisms may be suppression of the tumor suppressor RASSF4 by SPRR1B (Fig. 4E).

Human *RASSF4* binds to K-Ras in a GTP-dependent manner via the effector domain and synergizes with K-Ras to induce apoptotic cell death in 293T cells. Expression of *RASSF4* inhibits the growth of human tumor cells. *RASSF4* is broadly expressed in human tissues but is frequently down-regulated in human tumor cell lines and primary tumors. The expression RASSF4 correlates with methylation of the promoter. RASSF4 induces apoptosis in 293T cells in a Ras-associated manner [31,32]. Induction of apoptosis is considered to one of the mechanisms by which RASSF4 acts as a tumor suppressor. In this study, we found that RASSF4 suppresses the MAP kinase signal by suppression of ERK phosphorylation. Since RASSF4 has an RA domain and associates with Ras, RASSF4 may directly suppress the MAP kinase signal.

In summary, we successfully isolated OSCC CSCs/CICs by using the ALDEFLUOR assay. The *SPRR1B* gene was expressed more highly in the ALDH1^{br} population than in the ALDH1^{low} population and has a role in OSCC cell growth by suppression of the tumor suppressor RASSF4. Overexpression of SPRR1B might be related to carcinogenesis of OSCC and maintenance of OSCC CICs/CSCs.

Acknowledgments

The authors thank Dr Kitamura for kindly providing a retrovirus system. This work was supported by Grants-in-Aid for Scientific Research from the Ministry of Education, Culture, Sports, Science and Technology of Japan (Grant Nos. 16209013, 17016061 and 15659097) for Practical Application Research from the Japan Science and Technology Agency, and for Cancer Research (15–17 and 19–14) from the Ministry of Health, Labor and Welfare of Japan, Ono Cancer Research Fund (to N. S.) and Takeda Science Foundation (to Y. H.). This work was supported in part by the National Cancer Center Research and Development Fund (23-A-44).

Appendix A. Supplementary data

Supplementary data associated with this article can be found, in the online version, at http://dx.doi.org/10.1016/j.bbrc.2013.08.021.

References

[1] S. Warnakulasuriya, Global epidemiology of oral and oropharyngeal cancer, Oral Oncol. 45 (2009) 309–316.
[2] M.F. Clarke, J.E. Dick, P.B. Dirks, C.J. Eaves, C.H. Jamieson, D.L. Jones, J. Visvader, I.L. Weissman, G.M. Wahl, Cancer stem cells–perspectives on current status and future directions: AACR workshop on cancer stem cells, Cancer Res. 66 (2006) 9339–9344.
[3] C.T. Jordan, M.L. Guzman, M. Noble, Cancer stem cells, N. Engl. J. Med. 355 (2006) 1253–1261.
[4] C.Y. Park, D. Tseng, I.L. Weissman, Cancer stem cell-directed therapies: recent data from the laboratory and clinic, Mol. Ther. 17 (2009) 219–230.
[5] Y. Hirohashi, T. Torigoe, S. Inoda, A. Takahashi, R. Morita, S. Nishizawa, Y. Tamura, H. Suzuki, M. Toyota, N. Sato, Immune response against tumor antigens expressed on human cancer stem-like cells/tumor-initiating cells, Immunotherapy 2 (2010) 201–211.
[6] M.E. Prince, R. Sivanandan, A. Kaczorowski, G.T. Wolf, M.J. Kaplan, P. Dalerba, I.L. Weissman, M.F. Clarke, L.E. Ailles, Identification of a subpopulation of cells with cancer stem cell properties in head and neck squamous cell carcinoma, Proc. Natl. Acad. Sci. USA 104 (2007) 973–978.
[7] K. Kanki, T. Torigoe, I. Hirai, H. Sahara, K. Kamiguchi, Y. Tamura, A. Yagihashi, N. Sato, Molecular cloning of rat NK target structure – the possibility of CD44 involvement in NK cell-mediated lysis, Microbiol. Immunol. 44 (2000) 1051–1061.
[8] A. Okamoto, K. Chikamatsu, K. Sakakura, K. Hatsushika, G. Takahashi, K. Masuyama, Expansion and characterization of cancer stem-like cells in squamous cell carcinoma of the head and neck, Oral Oncol. 45 (2009) 633–639.
[9] A. Yoshida, Molecular genetics of human aldehyde dehydrogenase, Pharmacogenetics 2 (1992) 139–147.
[10] L. Armstrong, M. Stojkovic, I. Dimmick, S. Ahmad, P. Stojkovic, N. Hole, M. Lako, Phenotypic characterization of murine primitive hematopoietic progenitor cells isolated on basis of aldehyde dehydrogenase activity, Stem Cells 22 (2004) 1142–1151.
[11] D.A. Hess, T.E. Meyerrose, L. Wirthlin, T.P. Craft, P.E. Herrbrich, M.H. Creer, J.A. Nolta, Functional characterization of highly purified human hematopoietic repopulating cells isolated according to aldehyde dehydrogenase activity, Blood 104 (2004) 1648–1655.
[12] W. Matsui, C.A. Huff, Q. Wang, M.T. Malehorn, J. Barber, Y. Tanhehco, B.D. Smith, C.I. Civin, R.J. Jones, Characterization of clonogenic multiple myeloma cells, Blood 103 (2004) 2332–2336.
[13] D.A. Hess, L. Wirthlin, T.P. Craft, P.E. Herrbrich, S.A. Hohm, R. Lahey, W.C. Eades, M.H. Creer, J.A. Nolta, Selection based on CD133 and high aldehyde dehydrogenase activity isolates long-term reconstituting human hematopoietic stem cells, Blood 107 (2006) 2162–2169.
[14] D.J. Pearce, D. Taussig, C. Simpson, K. Allen, A.Z. Rohatiner, T.A. Lister, D. Bonnet, Characterization of cells with a high aldehyde dehydrogenase activity from cord blood and acute myeloid leukemia samples, Stem Cells 23 (2005) 752–760.
[15] C. Ginestier, M.H. Hur, E. Charafe-Jauffret, F. Monville, J. Dutcher, M. Brown, J. Jacquemier, P. Viens, C.G. Kleer, S. Liu, A. Schott, D. Hayes, D. Birnbaum, M.S. Wicha, G. Dontu, ALDH1 is a marker of normal and malignant human mammary stem cells and a predictor of poor clinical outcome, Cell Stem Cell 1 (2007) 555–567.
[16] Y.C. Chen, Y.W. Chen, H.S. Hsu, L.M. Tseng, P.I. Huang, K.H. Lu, D.T. Chen, L.K. Tai, M.C. Yung, S.C. Chang, H.H. Ku, S.H. Chiou, W.L. Lo, Aldehyde dehydrogenase 1 is a putative marker for cancer stem cells in head and neck squamous cancer, Biochem. Biophys. Res. Commun. 385 (2009) 307–313.

[17] S. Nishida, Y. Hirohashi, T. Torigoe, H. Kitamura, A. Takahashi, N. Masumori, T. Tsukamoto, N. Sato, Gene expression profiles of prostate cancer stem cells isolated by aldehyde dehydrogenase activity assay, J. Urol. 188 (2012) 294–299.

[18] T. Kuroda, Y. Hirohashi, T. Torigoe, K. Yasuda, A. Takahashi, H. Asanuma, R. Morita, T. Mariya, T. Asano, M. Mizuuchi, T. Saito, N. Sato, ALDH1-high ovarian cancer stem-like cells can be isolated from serous and clear cell adenocarcinoma cells, and aldh1 high expression is associated with poor prognosis, PLoS One 8 (2013) e65158.

[19] S. Inoda, Y. Hirohashi, T. Torigoe, M. Nakatsugawa, K. Kiriyama, E. Nakazawa, K. Harada, H. Takasu, Y. Tamura, K. Kamiguchi, H. Asanuma, T. Tsuruma, T. Terui, K. Ishitani, T. Ohmura, Q. Wang, M.I. Greene, T. Hasegawa, K. Hirata, N. Sato, Cep55/c10orf3, a tumor antigen derived from a centrosome residing protein in breast carcinoma, J. Immunother. 32 (2009) 474–485.

[20] S. Morita, T. Kojima, T. Kitamura, Plat-E: an efficient and stable system for transient packaging of retroviruses, Gene Ther. 7 (2000) 1063–1066.

[21] J. Nichols, B. Zevnik, K. Anastassiadis, H. Niwa, D. Klewe-Nebenius, I. Chambers, H. Scholer, A. Smith, Formation of pluripotent stem cells in the mammalian embryo depends on the POU transcription factor Oct4, Cell 95 (1998) 379–391.

[22] H. Niwa, Molecular mechanism to maintain stem cell renewal of ES cells, Cell Struct. Funct. 26 (2001) 137–148.

[23] I. Chambers, D. Colby, M. Robertson, J. Nichols, S. Lee, S. Tweedie, A. Smith, Functional expression cloning of Nanog, a pluripotency sustaining factor in embryonic stem cells, Cell 113 (2003) 643–655.

[24] K. Mitsui, Y. Tokuzawa, H. Itoh, K. Segawa, M. Murakami, K. Takahashi, M. Maruyama, M. Maeda, S. Yamanaka, The homeoprotein Nanog is required for maintenance of pluripotency in mouse epiblast and ES cells, Cell 113 (2003) 631–642.

[25] A. Cabral, A. Sayin, S. de Winter, D.F. Fischer, S. Pavel, C. Backendorf, SPRR4, a novel cornified envelope precursor: UV-dependent epidermal expression and selective incorporation into fragile envelopes, J. Cell Sci. 114 (2001) 3837–3843.

[26] J. Tesfaigzi, D.M. Carlson, Expression, regulation, and function of the SPR family of proteins. A review, Cell Biochem. Biophys. 30 (1999) 243–265.

[27] A. Cabral, P. Voskamp, A.M. Cleton-Jansen, A. South, D. Nizetic, C. Backendorf, Structural organization and regulation of the small proline-rich family of cornified envelope precursors suggest a role in adaptive barrier function, J. Biol. Chem. 276 (2001) 19231–19237.

[28] M. De Heller-Milev, M. Huber, R. Panizzon, D. Hohl, Expression of small proline rich proteins in neoplastic and inflammatory skin diseases, Br. J. Dermatol. 143 (2000) 733–740.

[29] D.H. Cho, Y.K. Jo, S.A. Roh, Y.S. Na, T.W. Kim, S.J. Jang, Y.S. Kim, J.C. Kim, Upregulation of SPRR3 promotes colorectal tumorigenesis, Mol. Med. 16 (2010) 271–277.

[30] Y. Tesfaigzi, P.S. Wright, S.A. Belinsky, SPRR1B overexpression enhances entry of cells into the G0 phase of the cell cycle, Am. J. Physiol. Lung Cell. Mol. Physiol. 285 (2003) L889–898.

[31] K. Eckfeld, L. Hesson, M.D. Vos, I. Bieche, F. Latif, G.J. Clark, RASSF4/AD037 is a potential ras effector/tumor suppressor of the RASSF family, Cancer Res. 64 (2004) 8688–8693.

[32] L. van der Weyden, D.J. Adams, The Ras-association domain family (RASSF) members and their role in human tumourigenesis, Biochim. Biophys. Acta 1776 (2007) 58–85.

Pathology International

Pathology International 2013; **63**: 391–397 doi:10.1111/pin.12079

Original Article

Expression of ECRG4 is associated with lower proliferative potential of esophageal cancer cells

Junichi Matsuzaki,[1] Toshihiko Torigoe,[1] Yoshihiko Hirohashi,[1] Yasuaki Tamura,[1] Hiroko Asanuma,[1] Emiri Nakazawa,[1] Eri Saka,[2] Kazuyo Yasuda,[1] Shuji Takahashi[1] and Noriyuki Sato[1]

[1]*Department of Pathology, Sapporo Medical University School of Medicine and* [2]*Sapporo Immunodiagnostic Laboratory, Sapporo, Japan*

We have shown that ECRG4 suppressed Fas-induced apoptosis in Jurkat cells. ECRG4 mRNA expression was ubiquitously detected in normal adult human tissues, suggesting that ECRG4 plays a major role in human tissues. ECRG4 mRNA expression was down-regulated in tumor cells. Expression of ECRG4 suppressed cell growth. We established an anti-ECRG4 monoclonal antibody. Our immunohistochemical analysis demonstrated that ECRG4-positive cells tended to be distributed in the region that was negative for Ki-67 in esophageal squamous cell carcinoma tissues. There was a significant inverse correlation between ECRG4 expression and Ki-67 labeling index in esophageal squamous cell carcinoma. This study provides the first functional evidence for an association of endogenous expression of ECRG4 with cell proliferation. ECRG4 is a candidate tumor suppressor gene that might be involved in the proliferation of esophageal squamous cell carcinoma.

Key words: esophageal cancer-related gene 4, esophageal squamous cell carcinoma, Ki-67 labeling index, tumor suppressor

In our recent study, we found that esophageal cancer-related gene 4 (ECRG4) was expressed in resting T-cells but was down-regulated in activated T-cells. Activated T-cells had increased sensitivity to Fas-induced apoptosis and increased proliferative capacity. The results suggested that ECRG4 was involved in reducing Fas-induced apoptosis and suppression of cell growth. Our study clarified that ECRG4 is a novel antiapoptotic gene that might be involved in negative regulation of caspase 8-mediated apoptosis in T-cells.[1] ECRG4 has also been identified as one of the down-regulated genes in esophageal cancer tissues.[2] ECRG4 is down-regulated via promoter hypermethylation in different types of human cancer cells.[3–6] Overexpression of ECRG4 results in suppression of cancer cell growth and inhibition of cancer cell migration and invasion.[7–8] High expression level of ECRG4 in patients with esophageal squamous cell carcinoma (ESCC) was associated with longer survival than that in patients with low ECRG4 expression level. However, the relationship between ECRG4 expression and cell proliferation in ESCC remains unclear.

In this study, we investigated the relationship between ECRG4 expression and proliferative capacity in ESCC using immunohistochemical staining with clinical samples.

MATERIALS AND METHODS

Cell lines and culture conditions

Human embryonic kidney cell line 293T, human gastric cancer cell line SNU1, human cervical adenocarcinoma cell line HeLa, and human T cell leukemia cell line Jurkat were obtained from American Type Culture Collection (Manassas, VA). Human oral cancer squamous cell carcinoma cell line HSC2 was obtained from the Human Science Research Resources Bank (HSRRB, Osaka, Japan). Human esophageal squamous cancer cell line TE8 was obtained from RIKEN Bioresource Center (Ibaraki, Japan). Human lung adenocarcinoma cell line 1–87 was obtained from the Cell Resource Center for Biomedical Research, Tohoku University (Sendai, Japan). Human colon adenocarcinoma cell lines Colo320 and SW480 were kind gifts from Dr Kohzoh Imai (Sapporo Medical University, Sapporo, Japan). Human

Correspondence: Toshihiko Torigoe, MD, PhD, Department of Pathology, Sapporo Medical University School of Medicine, South-1 West-17 Chuo-ku, Sapporo 060-8556, Japan. Email: torigoe @sapmed.ac.jp

Conflict of interest: The authors declare no conflict of interest.

Received 29 December 2012. Accepted for publication 25 June 2013.

esophageal squamous cancer cell line KE4 was kindly provided by Dr Kyogo Itoh (Kurume University Research Center for Innovation Cancer Therapy, Fukuoka, Japan). Human renal clear cell cancer cell line SMKT R-2 was a kind gift from Dr Noriomi Miyao (Sapporo Medical University, Sapporo, Japan). Human oral squamous cancer cell lines OSC19 and OSC20 and human lung adenocarcinoma cell line LHK2 were established in our laboratory. These cells, except for Jurkat cells, were cultured in DMEM (Sigma-Aldrich, St. Louis MO) with 10% heat-inactivated fetal bovine serum (FBS), 100 U/mL penicillin G and 100 μg/mL streptomycin. Human T cell leukemia cell line Jurkat cells were cultured in RPMI1640 (Sigma-Aldrich) with 10% heat-inactivated fetal bovine serum (FBS), 100 U/mL penicillin G and 100 μg/mL streptomycin. The Fas-resistant Jurkat variant clone (Jurkat-FasR) was established and characterized previously.[9]

Reverse transcription-PCR

The cDNA mixture was synthesized by reverse transcription using SuperScript III and oligo(dT) primer (Invitrogen) according to the manufacturer's protocol. For detection of mRNA expression, we performed RT-PCR as follows. Briefly, PCR amplification was done in 25 μL PCR mixture containing 1 μL of the cDNA mixture, KOD DASH DNA polymerase (Toyobo, Osaka, Japan), and 200 pmol of a primer. The PCR mixture was initially incubated at 94°C for 5 min followed by 30 cycles of denaturation at 94°C for 30 s, annealing at 60°C for 2 s and extension at 74°C for 30 s. For specific detection of ECRG4, the primer pair used for RT-PCR analysis was 5'-AAACGAGAAGCACCTGTTCC-3' and 5'-GTAGTTGACG CTGGCTCCAT-3' as forward and reverse primers, respectively. As an internal control, glyceraldehyde-3-phosphate dehydrogenase (GAPDH) was detected by using forward primer 5'-CGAGATCCCTCCAAAATCAA-3' and reverse primer 5'-GTCTTCTGGGTGGCAGTGAT-3'.

Cell proliferation assay

Briefly, cells were suspended at a concentration of 0.5–2 × 10^4 cells in 100 μL of culture medium per well on 96-well flat-bottom plates (Corning, NY) for 24–96 h. Then a 1/10 volume of Premix WST-1 (Takara) was added to each well and the plates were incubated at 37°C for 2 to 4 h. The optical density of each well was quantified by using a microplate reader (Model 680 microplate reader, Bio-Rad). The test wavelength was 450 nm and the reference one was 655 nm. For the MTT assay, cells were incubated with MTT reagent (Sigma) for 4 h, and formazan dye was solubilized by the addition of acidic isopropanol. The test wavelength was 570 nm and the reference one was 630 nm.

Plasmids and transfection

To construct expression plasmids, total RNA was extracted from the Fas-resistant Jurkat clone, and cDNA was synthesized from the RNA by reverse transcription. Full-length ECRG4 (GenBank: AF325503.1) with an NH2-terminal myc epitope tag was amplified by using specific forward and reverse primers including *Nhe*I and *Xho*I restriction sites. The PCR product was purified and cloned into mammalian expression vector pcDNA3.1 (Invitrogen, Carlsbad, CA). Full-length ECRG4 with a COOH-terminal flag epitope tag was amplified by using specific forward and reverse primers including *Bam*HI and *Xho*I restriction sites and cloned into mammalian expression vector pcDNA3.1. Similarly, the PCR product of full-length ECRG4 with an NH2-terminal flag epitope tag was produced and cloned into *Nhe*I and *Xho*I restriction sites of the pcDNA3.1 vector. 293T cells were transfected by using Lipofectamine 2000 reagent (Invitrogen). For the construct of protein expression, an N-terminal deletion mutant of ECRG4 cDNA was inserted into the pQE30 (QIAGEN) vector, which allows the expression of recombinant proteins with an NH2-terminal His6 tag, at the *Bam*HI and *Sal*I sites. The primer pair was 5'-CGCGGATCCCGAGAAGCACCTGTTCCAACT-3' as a forward primer and 5'-ACGCGTCGACTTAGTAGTCATCG TAGTTGAC-3' as a reverse primer (underlines indicating *Bam*HI and *Sal*I recognition sites, respectively). The cDNA sequences were confirmed by direct sequencing.

Tissue samples

Tissue specimens were described previously.[1] They were obtained from an esophageal cancer patient who underwent surgery at Kushiro City General Hospital. Tumor tissues and corresponding normal tissues were frozen at –80°C. The patient and family gave informed consent for the use of tissue specimens in research.

Western blotting

Cell lysate with radioimmunoprecipitation assay buffer (150 mmol/L NaCl, 1.0% NP40, 0.5% deoxycholic acid, 0.1% SDS, 50 mmol/L Tris-HCl (pH 8.0), protease inhibitor cocktail (Complete, Roche Diagnostics, Basel, Switzerland)) were boiled with SDS sample buffer and then separated by 12.5% or 15% SDS-PAGE. The proteins were transferred electrophoretically to a polyvinylidene fluoride membrane (Immunobilon-P, Millipore, Billerica, MA) and probed with

mouse anti-FLAG m2 (Sigma-Aldrich), mouse anti-myc 9E10, or mouse anti-β-actin mAb AC-15 (Sigma-Aldrich). After three washes with wash buffer (0.1% Tween 20, PBS), the membrane was reacted with a peroxidase-labeled secondary antibody (peroxidase-labeled goat anti-mouse IgG; KPL, Gaithersburg, MD). Finally, the signal was visualized by using an enhanced chemiluminescence detection system (Amersham Life Science, Arlington Heights, IL) according to the manufacturer's protocol.

Establishment of anti-ECRG4 monoclonal antibody

To characterize the expression of endogenous ECRG4, we established mouse antiserum against ECRG4 as described previously.[10] N-terminal deletion mutant of ECRG4 (aa41-148) recombinant protein (100 μg) was used for immunization of BALB/c mice by intraperitoneal (i.p.) injection four times at 2-week intervals. One week after the last injection, spleen cells were collected and fused with the NS-1 mouse myeloma cell line (ATCC) at a 4:1 ratio. All mouse procedures were carried out in accordance with institutional protocol guidelines at Sapporo Medical University School of Medicine. Screening was performed with ELISA using recombinant N-terminal deletion mutant of ECRG4 protein and Western blotting.

Immunohistochemical staining

Immunohistochemical staining was done on formalin-fixed, paraffin-embedded sections as described previously.[11] Four- to 5-μm-thick sections were cut, deparaffinized in xylene, and rehydrated in graded alcohol. Antigen retrieval was done by boiling for 20 min in a microwave oven in a preheated 0.01 mol/L concentration of sodium citrate buffer (pH 6.0). Endogenous peroxidase activity was blocked by 3% hydrogen peroxide in ethanol for 5 min. Slides were incubated for 1 h with the mAb: anti-ECRG4 and anti-Ki67 (clone BGX-Ki-67, Biogenex, Fremont, CA). After incubation, the slides were washed thrice with PBS and incubated for 30 min with Simple Stain MAX-PO (Multi) secondary antibody mixture (Nichirei, Tokyo, Japan). After washing thrice with PBS, staining was done by incubation for 1 to 2 min with 3,3'-diaminobenzidine used as the chromogen, and counterstaining was done with Mayer's hematoxylin.

Statistical analysis

Statistical differences between groups were evaluated using a two-tailed unpaired-*t* test or a two-tailed Mann-Whitney U-test or the chi square test and ANOVA, with *P*-values <0.05 considered significant.

RESULTS

Overexpression of ECRG4 suppresses cell growth

First, cell growth rates were assessed and the growth rates of Jurkat-FasR and parental Jurkat cells were compared. Jurkat-FasR cells showed decreased proliferative capacity (Fig. 1a). Since ECRG4 is one of the genes overexpressed in

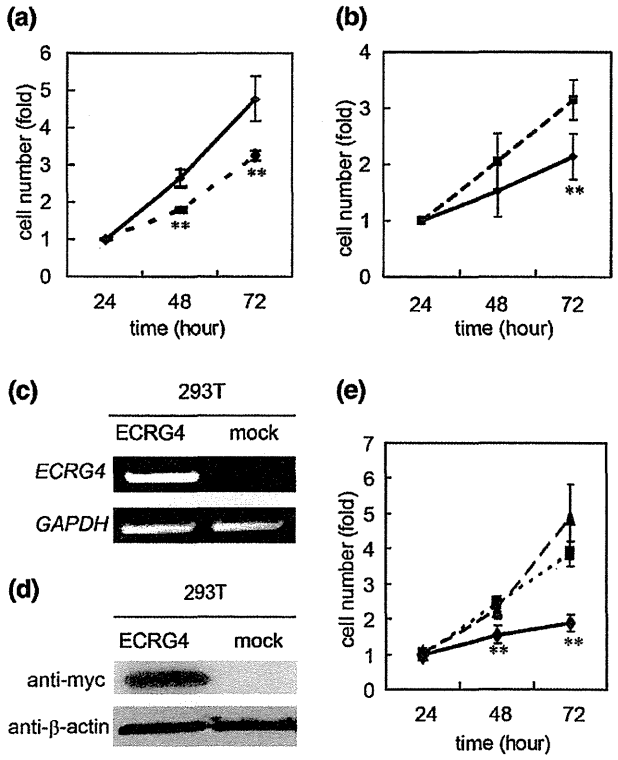

Figure 1 (**a**) ECRG4 expression suppresses cell growth. Parental Jurkat cells and Jurkat-FasR cells (2×10^3) were plated on 96-well tissue culture dishes. The relative cell numbers were assessed at 24, 48, 72 h after plating by WST-1 assay. (cell number at 24 h = 1.0). The data represent averages of triplicate samples and standard deviation. **, $P < 0.01$, unpaired *t*-test. (**b**) Stable ECRG4-expressing Jurkat (Jurkat-ECRG4) cells were established by transfection with the plasmid pIRESpuro3-ECRG4-FLAG and puromycin selection. Jurkat-mock cells were established by transfection with the mock plasmid vector pIRESpuro3. Parental Jurkat cells and Jurkat transfectants (2×10^3) were plated on 96-well tissue culture dishes. The relative cell numbers were assessed at 24, 48, 72 h after plating by WST-1 assay. (cell number at 24 h = 1.0). The data represent averages of triplicate samples and standard deviation. **, $P < 0.01$, unpaired *t*-test. (**c,d**) 293T cells were transfected with the pcDNA3.1-myc-ECRG4 expression vector or pcDNA3.1-myc expression vector. (**e**) Parental 293T cells (293T-WT) and the transfectants (2×10^3) were plated on 96-well tissue culture dishes. The relative cell numbers were assessed at 24, 48, 72 h after transfection by MTT assay. (cell number at 24 h = 1.0). The data represent averages of triplicate samples and standard deviation. **, $P < 0.01$, ANOVA. —•—, Jurkat; - • -, Jurkat-FasR; —▪—, ECRG4; - ▪ -, Mock; —▲—, ECRG4; - ▲ -, Mock; —▲—, WT.

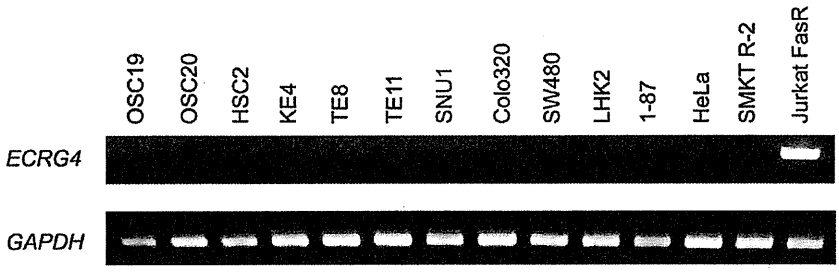

Figure 2 ECRG4 mRNA expression in various cancer cells. cDNA samples from various cancer cell lines were analyzed for the expression of ECRG4 and GAPDH by RT-PCR with specific primers.

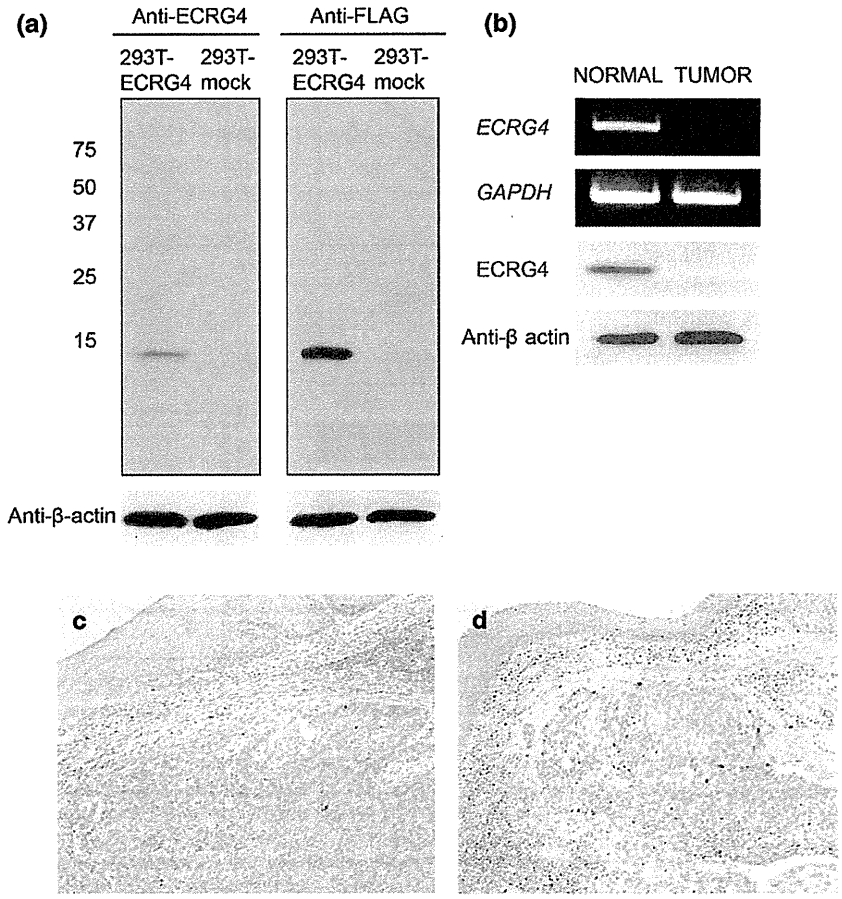

Figure 3 Establishment of anti-ECRG4 monoclonal antibody and immunohistochemical staining with the specific antibody. (**a**) 293T cells were transfected with the pcDNA3.1-ECRG4-FLAG expression vector. The transfected cells were characterized by Western blotting with anti-ECRG4 monoclonal antibody, anti-FLAG tag antibody and anti-β-actin antibody. (**b**) Expression of ECRG4 was determined by RT-PCR and Western blotting in tissue pairs of noncancerous tissue (Normal) and carcinoma tissue (Tumor) in an esophageal cancer patient. Immunohistochemical staining (x100) showed (**c**) ECRG4-positive staining and (**d**) ECRG4-negative staining.

Jurkat-FasR cells, we established stable ECRG4-expressing cells by gene transfection. Jurkat-mock cells were established by transfecting the plasmid vector pIRESpuro3 into Jurkat cells as described previously.[1] Jurkat-ECRG4 cells had a significantly slower growth rate than that of the control cells (Fig. 1b). Next, we examined proliferative capacity of 293T cells. ECRG4-negative 293T cells were transfected with a plasmid encoding myc-tagged ECRG4, and the resulting 293T-ECRG4 cells transiently expressed the mRNA and protein (Fig. 1c,d). Cell growth rates were assessed and compared among parental 293T cells (293T-WT), 293T-mock transfectant cells and 293T-ECRG4 cells. 293T-ECRG4 cells had a significantly slower growth rate than that of the control cells (Fig. 1e). These findings suggested that ECRG4 might be involved in cell growth as well as Fas-induced apoptotic signals.

Expression of ECRG4 mRNA in tumor cell lines

ECRG4 mRNA expression was investigated in human tumor cell lines (3 oral cancers, 3 esophageal cancers, 1 gastric cancer, 2 colon cancers, 2 lung cancers, 1 cervical cancer, 1

renal cell cancer). ECRG4 mRNA expression was down-regulated in all human tumor cell lines (Fig. 2).

Establishment of anti-ECRG4 monoclonal antibody

Next, we examined whether a decrease in endogenous ECRG4 level alters cell growth. In order to evaluate the endogenous ECRG4 protein expression level, we established an anti-ECRG4 monoclonal antibody (Fig. 3a). We examined ECRG4 protein expression level in an esophageal cancer patient. ECRG4 was down-regulated in esophageal cancer tissues compared with the levels in normal tissues (Fig. 3b). Next, we examined ECRG4 protein levels in formalin-fixed, paraffin-embedded esophageal squamous cell carcinoma specimens by immunohistochemical staining. ECRG4 immunoreactivity was evaluated qualitatively. Since ECRG4 was cloned from the normal esophageal epithelium, cases in which ECRG4 immunoreactivity in the tumor tissues was the same as that in the normal esophageal epithelium were defined as positive (Fig. 3c). ECRG4 was distributed in the cytoplasm. Cases in which ECRG4 immunoreactivity in the tumor tissues was less than that in the normal esophageal epithelium were defined as negative (Fig. 3d).

Histopathological analysis of ECRG4 expression and cell growth

Since ECRG4 suppressed growth of cultured cells, we examined whether the ECRG4 protein level affects proliferative capacity of esophageal squamous cell carcinoma cells. We examined the relationship in esophageal squamous cell carcinoma tissues between ECRG4 expression and Ki-67 labeling index. Clinicopathological data for 10 patients diagnosed with ESCC are summarized in Table 1. There were no significant differences between the ECRG4 negative group and ECRG4 positive group. In esophageal squamous cell carcinoma tissues, ECRG4-positive cells tended to be distributed in the region that was negative for Ki-67 in many, but not all, cases examined (Fig. 4a–d). Our immunohistochemical analysis demonstrated a significant inverse correlation between ECRG4 expression and Ki-67 labeling index in esophageal squamous cell carcinoma (Fig. 4e). Results of immunohistochemical staining for the 10 patients diagnosed with ESCC are summarized in Table 2. Furthermore, we confirmed that there was no correlation between ECRG4 positivity and Ki-67 positivity using high magnification data with serial sections (Fig. S1).

Table 1 Association between esophageal cancer-related gene 4 (ECRG4) expression and clinicopathological characteristics of patients with esophageal squamous cell carcinoma (ESCC)

Characteristics	ECRG4 Positive $n = 5$	ECRG4 Negative $n = 5$	*P*-value
Age, y			0.20
≤60	3	1	
>60	2	4	
Sex			0.30
Male	4	5	
Female	1	0	
Tumor status			0.72
T1	1	1	
T2	2	1	
T3	2	2	
T4	0	1	
Lymph node metastasis			0.57
N0	1	0	
N1	3	3	
N2	1	1	
N3	0	1	
Stage			0.50
I	1	0	
II	2	1	
III	2	2	
IVa	0	1	
IVb	0	1	
Tumor cell differentiation			0.28
Good	2	0	
Moderate	2	3	
Poor	1	2	

Chi square test.

DISCUSSION

We have shown that ECRG4-negative ESCC has high proliferative capacity by using clinical samples obtained from surgical resections. We previously reported that ECRG4 was a novel antiapoptotic protein and that it suppressed the activation of caspase 8.[1] The ECRG4 gene was previously cloned from human normal esophageal epithelium and identified as one of the down-regulated genes in esophageal squamous cell carcinoma tissues.[2] The mechanism of inactivation of this gene in tumor tissues involves promoter hypermethylation, which is a frequent molecular event in esophageal squamous cell carcinoma.[3] We previously reported ECRG4 expression in normal adult tissues and tumor tissues. ECRG4 mRNA expression was detected ubiquitously in normal adult tissues, and expression of ECRG4 mRNA was investigated in several pairs of tumor tissues and corresponding normal tissues derived from surgical specimens of the same patient (1 esophageal cancer, 4 gastric cancers, 4 colon cancers, 2 liver cancers, and 2 kidney cancers). ECRG4 mRNA expression was down-regulated in 11 of the 13 stomach, kidney, esophagus and colon tumor tissues.[1] ECRG4 mRNA expression is decreased in esophageal cancer cells, gastric cancer cell lines, colorectal cancer cells and glioma cells.[3,4,6] Our data showed that ECRG4 mRNA expression was decreased in many other types of human cancer cell lines including oral cancer, esophageal cancer, gastric cancer, colorectal cancer, lung cancer, cervical cancer and renal cancer cell lines. ECRG4 contains a

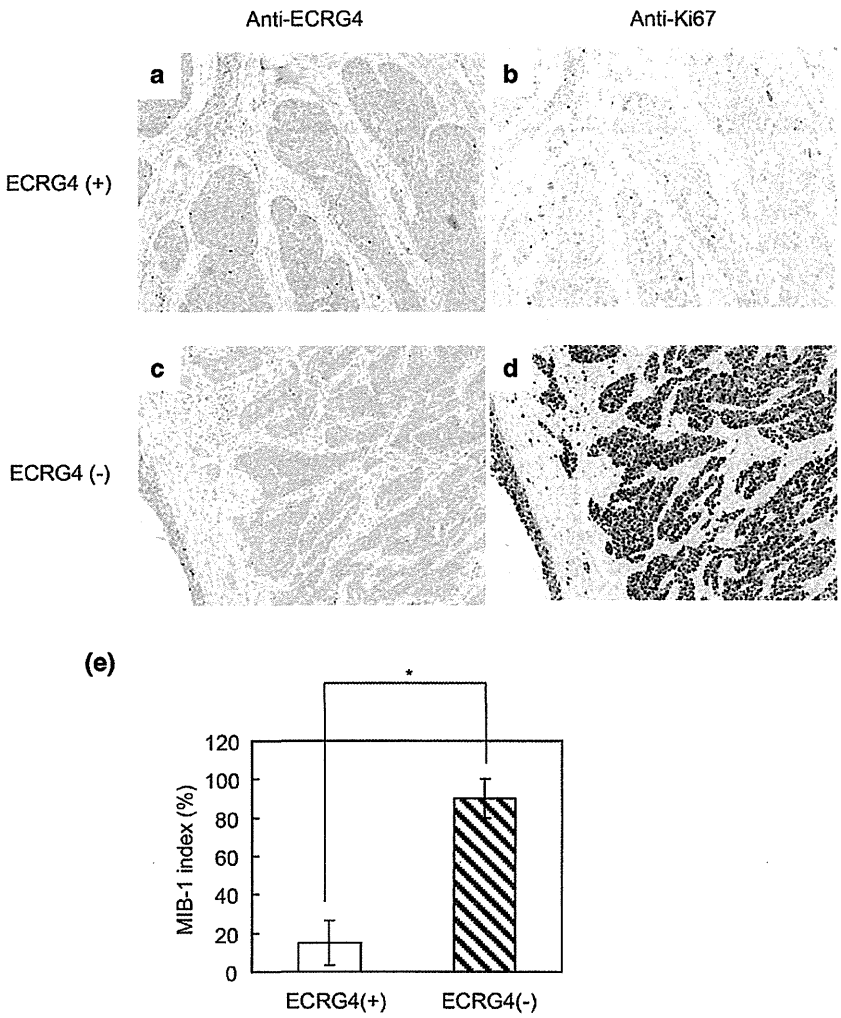

Figure 4 Inverse relationship of the immunoreactivity between ECRG4 and Ki67. Immunohistochemical staining of anti-ECRG4 and anti-Ki67 (x100). (**a,b**) ECRG4-positive staining case. (**c,d**) ECRG4-negative staining case. (**e**) Ki-67 labeling indexes of ECRG4-positive and -negative cases. Each value is the median and standard error of the mean. *, $P<0.05$, Mann-Whitney U-test.

Table 2 Correlation between esophageal cancer-related gene 4 (ECRG4) expression and esophageal squamous cell carcinoma (ESCC) clinicopathological features

Case	Age	Gender	Differentiation	pT	INF	pN	Ly	v	Stage	ECRG4	Ki-67
1	70	male	good	T3	INFb	N2	ly1	V0	III	+	+++
2	50	male	good	T3	INFb	N1	ly2	v1	III	+	–
3	51	male	moderate	T2	INFb	N1	ly2	v2	II	+	–
4	58	male	poor	T2	INFb	N1	ly0	v0	II	+	–
5	69	female	moderate	T1b	INFa	N0	ly0	v0	I	+	–
6	59	male	poor	T2	INFc	N1	ly3	v0	IVb	–	+++
7	62	male	moderate	T4	INFb	N1	ly1	v1	IVa	–	+
8	73	male	moderate	T3	INFb	N1	ly2	v0	III	–	++
9	70	male	moderate	T3	INFb	N3	ly0	v1	III	–	+++
10	67	male	poor	T1b	INFa	N2	ly1	v0	II	–	+++

CDC45 homology domain that overlaps with the APC10 homology domain in the middle region of the protein.[1] Since CDC45 and APC10 homolog domains are cell cycle control domains, ECRG4 might be involved in cell growth. It has been shown that exogenous ECRG4 suppresses cell growth.[4,6–8] Our data also showed that exogenous ECRG4 suppressed proliferation of Jurkat cells and 293T cells. However, the relationship between endogenous ECRG4 expression and cell proliferation remains unclear. To clarify the relationship between endogenous ECRG4 expression and cell proliferation, we established an anti-ECRG4 monoclonal antibody.

Our immunohistochemical staining results demonstrated that downregulation of endogenous ECRG4 was associated with high proliferative capacity of ESCC cells. ECRG4 protein expression has been shown to be associated with primary tumor size, regional lymph node metastasis, and tumor stage in ESCC in Chinese patients.[8] Similarly, ECRG4 mRNA expression level in patients with locally invasive T2-4 tumors was significantly lower than that in the less invasive T1 tumors, and the levels in stage 4 tumors was significantly lower than the levels in tumors in stages 0–3. However, ECRG4 mRNA expression levels were not significantly different with respect to lymph node status in Japanese patients.[12] Ethnic variations in tumor biology have been reported.[13,14] Our clinicopathological characteristics were no significant differences in primary tumor size (T1-3 versus T4, $P = 0.29$), regional lymph node metastasis (N0-1 versus N2-3, $P = 0.49$), and tumor stage (stages 1–3 versus stage 4, $P = 0.11$) in ESCC. With respect to tumor size and tumor stage, the small population of our study might be the reason for the observed statistically insignificant. However, with respect to regional lymph node metastasis, no significant differences might be due to ethnicity of the patients. Since a high expression level of ECRG4 in patients with ESCC is associated with longer survival than that in patients with low ECRG4 expression level,[12] ECRG4 expression is a candidate prognostic marker for ESCC. Therefore, our anti-ECRG4 antibody might contribute to prediction of the prognosis for patients with ESCC.

In conclusion, the present clinicopathological study clarified the relationship between ECRG4 expression and cell proliferation capacity in ESCC. Our results indicate that ECRG4 staining might be a good clinicopathological prognostic marker for patients with ESCC.

ACKNOWLEDGMENT

This work was supported by grants from the Ministry of Education, Culture, Sports, Science and Technology of Japan.

REFERENCES

1 Matsuzaki J, Torogoe T, Hirohashi Y *et al.* ECRG4 is a novel inhibitor of Fas-induced apoptosis in human T-leukemia cells. *Carcinogenesis* 2012; **33**: 996–1003.
2 Su T, Liu H, Lu S. Cloning and identification of cDNA fragments related to human esophageal cancer. *Zhonghua Zhong Liu Za Zhi* 1998; **20**: 254–7 [in Chinese].
3 Yue CM, Deng DJ, Bi MX, Guo LP, Lu SH. Expression of ECRG4, a novel esophageal cancer-related gene, downregulated by CpG island hypermethylation in human esophageal squamous cell carcinoma. *World J Gastroenterol* 2003; **9**: 1174–8.
4 Götze S, Feldhaus V, Traska T *et al.* ECRG4 is a candidate tumor suppressor gene frequently hypermethylated in colorectal carcinoma and glioma. *BMC Cancer* 2009; **9**: 447.
5 Vanaja DK, Ehrich M, Van den Boom D *et al.* Hypermethylation of genes for diagnosis and risk stratification of prostate cancer. *Cancer Invest* 2009; **27**: 549–60.
6 Li W, Liu X, Zhang B *et al.* Overexpression of candidate tumor suppressor ECRG4 inhibits glioma proliferation and invasion. *J Exp Clin Cancer Res* 2010; **29**: 1–7.
7 Kujuro Y, Suzuki N, Kondo T. Esophageal cancer-related gene 4 is a secreted inducer of cell senescence expressed by aged CNS precursor cells. *Proc Natl Acad Sci U S A* 2010; **107**: 8259–64.
8 Li LW, Yu XY, Yang Y, Zhang CP, Guo LP, Lu SH. Expression of esophageal cancer related gene 4 (ECRG4), a novel tumor suppressor gene, in esophageal cancer and its inhibitory effect on the tumor growth in vitro and in vivo. *Int J Cancer* 2009; **125**: 1505–13.
9 Takahashi S, Sato N, Takayama S *et al.* Establishment of apoptosis-inducing monoclonal antibody 2D1 and 2D1-resistant variants of human T cell lines. *Eur J Immunol* 1993; **23**: 1935–41.
10 Inoda S, Hirohashi Y, Torigoe T *et al.* Cep55/c10orf3, a tumor antigen derived from a centrosome residing protein in breast carcinoma. *J Immunother* 2009; **32**: 474–85.
11 Asanuma H, Torigoe T, Kamiguchi K *et al.* Survivin expression is regulated by coexpression of human epidermal growth factor receptor 2 and epidermal growth factor receptor via phosphatidylinositol 3-kinase/AKT signaling pathway in breast cancer cells. *Cancer Res* 2005; **65**: 11018–25.
12 Mori Y, Ishiguro H, Kuwabara Y *et al.* Expression of ECRG4 is an independent prognostic factor for poor survival in patients with esophageal squamous cell carcinoma. *Oncol Rep* 2007; **18**: 981–5.
13 Bashash M, Hislop TG, Shah AM, Le N, Brooks-Wilson A, Bajdik CD. The prognostic effect of ethnicity for gastric and esophageal cancer: The population-based experience in British Columbia, Canada. *BMC Cancer* 2011; **11**: 164.
14 Bhoo-Pathy N, Hartman M, Yip CH *et al.* Ethnic differences in survival after breast cancer in South East Asia. *PLoS One* 2012; **7**: e30995.

SUPPORTING INFORMATION

Additional Supporting Information may be found in the online version of this article at the publisher's web-site:

Figure S1 Correlation between ECRG4 positivity and Ki67 positivity in an ECRG4-positive staining case. High magnification data (x400) with serial sections using anti-ECRG4 (A) and anti-Ki67 (B).

OPEN ACCESS Freely available online

PLOS ONE

Ovarian Cancer Stem Cells Are Enriched in Side Population and Aldehyde Dehydrogenase Bright Overlapping Population

Kazuyo Yasuda[1], Toshihiko Torigoe[1]*, Rena Morita[1], Takahumi Kuroda[1], Akari Takahashi[1], Junichi Matsuzaki[1], Vitaly Kochin[1], Hiroko Asanuma[2], Tadashi Hasegawa[2], Tsuyoshi Saito[3], Yoshihiko Hirohashi[1]*, Noriyuki Sato[1]

1 Department of Pathology, Sapporo Medical University School of Medicine, Chuo-Ku, Sapporo, Japan, **2** Department of Surgical Pathology, Sapporo Medical University School of Medicine, Chuo-Ku, Sapporo, Japan, **3** Department of Obstetrics and Gynecology, Sapporo Medical University School of Medicine, Chuo-Ku, Sapporo, Japan

Abstract

Cancer stem-like cells (CSCs)/cancer-initiaiting cells (CICs) are defined as a small population of cancer cells that have self-renewal capacity, differentiation potential and high tumor-initiating ability. CSCs/CICs of ovarian cancer have been isolated by side population (SP) analysis, ALDEFLUOR assay and using cell surface markers. However, these approaches are not definitive markers for CSCs/CICs, and it is necessary to refine recent methods for identifying more highly purified CSCs/CICs. In this study, we analyzed SP cells and aldehyde dehydrogenese bright ($ALDH^{Br}$) cells from ovarian cancer cells. Both SP cells and $ALDH^{Br}$ cells exhibited higher tumor-initiating ability and higher expression level of a stem cell marker, *sex determining region Y-box 2 (SOX2)*, than those of main population (MP) cells and $ALDH^{Low}$ cells, respectively. We analyzed an SP and $ALDH^{Br}$ overlapping population (SP/$ALDH^{Br}$), and the SP/$ALDH^{Br}$ population exhibited higher tumor-initiating ability than that of SP cells or $ALDH^{Br}$ cells, enabling initiation of tumor with as few as 10^2 cells. Furthermore, SP/$ADLH^{Br}$ population showed higher sphere-forming ability, cisplatin resistance, adipocyte differentiation ability and expression of *SOX2* than those of SP/$ALDH^{Low}$, MP/$ALDH^{Br}$ and MP/$ALDH^{Low}$ cells. Gene knockdown of SOX2 suppressed the tumor-initiation of ovarian cancer cells. An SP/$ALDH^{Br}$ population was detected in several gynecological cancer cells with ratios of 0.1% for HEC—1 endometrioid adenocarcinoma cells to 1% for MCAS ovary mucinous adenocarcinoma cells. Taken together, use of the SP and $ALDH^{Br}$ overlapping population is a promising approach to isolate highly purified CSCs/CICs and SOX2 might be a novel functional marker for ovarian CSCs/CICs.

Citation: Yasuda K, Torigoe T, Morita R, Kuroda T, Takahashi A, et al. (2013) Ovarian Cancer Stem Cells Are Enriched in Side Population and Aldehyde Dehydrogenase Bright Overlapping Population. PLoS ONE 8(8): e68187. doi:10.1371/journal.pone.0068187

Editor: Shannon M. Hawkins, Baylor College of Medicine, United States of America

Received December 17, 2012; **Accepted** May 28, 2013; **Published** August 13, 2013

Funding: This work was supported by Grants-in-Aid for Scientific Research from the Ministry of Education, Culture, Sports, Science and Technology of Japan (grant Nos. 16209013, 17016061 and 15659097) for Practical Application Research from the Japan Science and Technology Agency, and for Cancer Research (15-17 and 19-14) from the Ministry of Health, Labor and Welfare of Japan, Ono Cancer Research Fund (to NS) and Takeda Science Foundation (to YH). This work was supported in part by the National Cancer Center Research and Development Fund (23-A-44). The funders had no role in study design, data collection and analysis, decision to publish, or preparation of the manuscript.

Competing Interests: The authors have declared that no competing interests exist.

* E-mail: torigoe@sapmed.ac.jp (TT); hirohash@sapmed.ac.jp (YH)

Introduction

Cancer stem-like cells (CSCs)/cancer-initiating cells (CICs) are defined as small population of cancer cells that have the properties of high tumor initiating ability, self-renewal ability and differentiation ability [1–3]. Furthermore, CSCs/CICs are shown to be resistant to standard cancer therapies including chemotherapy and radiotherapy; therefore, CSCs/CICs are responsible for cancer relapse after treatment [4,5]. Several approaches have been described to identify CSCs/CICs, including isolation by CSC/CIC-specific cell surface marker expression (e.g. CD44, CD133, CD166), detection of side population (SP) cell phenotype by Hoechst 33342 exclusion and detection of aldehyde dehydrogenase 1 (ALDH1) activity in the ALDEFLUOR assay [6]. However, the expression of cell surface markers, SP cells and the expression of ALDH1 are not related to tumor-initiating ability in some reports [7–9]. These observations thus suggest that these stem cell markers (cell surface markers, SP cells and ALDH1) are not functional and not necessary for maintenance of CSCs/CICs. These markers may not define high tumorigenic CSCs/CICs, and these markers are thus merely surrogate markers for CSCs/CICs. Therefore, functional non-surrogate marker which is essential for maintenance of CSCs/CICs is expected.

Ovarian cancer is one of the major malignancies and causes the death of more than one million people in the world every year [10]. In addition, most patients have miserable episodes of ascites, especially in advanced stages. To improve the clinical treatment of ovarian cancer, ovarian cancer stem cell research has emerged as a recent topic. CD44 cell surface marker, SP cells and $ALDH^{Br}$ cells have been reported as stem cell markers for gynecological malignancies using cell lines OVCAR3, HEC-1 and other lines and primacy samples [11–14], and CSC/CIC research may improve the outcome of advanced ovarian cancer patients.

To improve the methods for isolation of highly purified ovarian CSCs/CICs, we analyzed the combination of known ovarian CSC/CIC markers. We analyzed ovarian cancer cell lines by SP analysis and ALDEFLUOR assay and found that SP cells and $ALDH^{Br}$ cells were higher tumorigenic than those of main population (MP) cells and $ALDH^{Low}$ cells, respectively. We found that the overlapping population of SP cells and $ALDH^{Br}$ cells (SP/$ALDH^{Br}$) were more highly tumorigenic. And we found that *SOX2* was expressed in an SP/$ALDH^{Br}$ population at higher level, and gene knockdown of *SOX2* abrogated the tumor-initiation of ovarian cancer cells. Therefore, SOX2 might be a novel functional marker for ovarian CSCs/CICs and SP/$ALDH^{Br}$ population is more suitable population for analysis of ovarian CSCs/CICs than SP cells or $ALDH^{Br}$ cells.

Materials and Methods

Ethics Statement

Mice were maintained and experimented on in accordance with the guidelines of and after approval by the Committee of Sapporo Medical University School of Medicine, Animal Experimentation Center under permit number 08-006. Any animal found unhealthy or sick were promptly euthanized. Immunohistochemical staining study was approved by Institutional Review Boards (IRB) of Sapporo Medical University Hospital. We obtained written informed consent from all patients according to the guidelines of the Declaration of Helsinki.

Cell lines and culture

Human ovarian cell lines (MCAS, HTBoA, OVCAR3, OVSAHO) and human endometrial carcinoma (HEC-1) cells were obtained from ATCC (Manassas, VA, USA). MCAS and HEC-1 cells were maintained in Minimun Essential medium (MEM) (Life Technologies, Grand Island, NY, USA). HTBoA and OVCAR3 cells were maintained in Dulbecco's modified Eagle's medium (DMEM) (Sigma-Aldrich, St Louis, MO, USA). OVSAHO cells were maintained in RPMI1640 medium (Sigma-Aldrich). Each cell line was supplemented with 10% FBS and cultured in a humidified 5% CO_2 incubator at 37°C.

Side population (SP) assay

Side population (SP) analysis was performed as described previously with some modifications [15,16]. Hoechst 33342 (Lonza, Walkersville, MD, USA) dye was used at the concentration of 2.5 or 5.0 μg/ml in the presence or absence of verapamil (50 mM; Sigma-Aldrich) as an inhibitor of the ABC transporter. The cells were incubated at 37°C for 60 min or 90 min with continuous shaking. One million of stained cells were analyzed by FACS Aria II (BD Biosciences, San Jose, CA, USA). The Hoechst 33342 dye was excited at 357 nm and its fluorescence was analyzed using dual wave-lengths (blue, 402–446 nm; red, 650–670 nm).

ALDEFLUOR assay

Aldehyde dehydrogenase (ALDH) activity was detected using an ALDEFLUOR assay kit (StemCell Technologies) according to the manufacturer's protocol [17]. Cells were stained by bodipy-aminoacetaldehyde (BAAA) at 1.5 mM and incubated for 30 min at 37°C. An inhibitor of ALDH1, diethylamino- benzaldehyde (DEAB), at a10-fold molar excess was used as a negative control. One million of stained cells were analyzed by FACS Aria II. The brightly fluorescent ALDH1-expressing cells ($ALDH1^{Br}$) were detected in the green fluorescence channel (520–540 nm).

SP and ALDEFLUOR dual staining

The cells were stained by Hoechst 33342 dye and then stained by BAAA. One million of SP and ALDEFLUOR-dual-stained cells were analyzed by FACS Aria II. The cells were divided into three groups according to ALDH intensity ($ALDH^{Br}$ (ALDH bright), $ALDH^{Mid}$ (ALDH middle), $ALDH^{Low}$ (ALDH low)), then analyzed by SP assay.

Immunohistochemical staining

Immunohistochemical staining using formalin-fixed paraffin-embedded sections of surgically resected ovarian carcinoma tissue was performed as described previously [18]. Anti-ALDH1 mouse antibody was used at 250-times dilution. Anti-ABCG2 rabbit polyclonal antibody (Sigma-Aldrich) was used at 5 μg/ml. Peroxidase-labeled goat anti-rabbit polyclonal antibody (Nichirei, Tokyo, Japan) was used as manufacturer's protocol and visualized by DAB. Alkaline phosphatase-labeled goat anti-mouse polyclonal antibody (Nichirei) was used as manufacturer's protocol and visualized by New Fuchsin (Nichirei). Membrane brown staining was judged as positive staining for ABCG2, and cytoplasm red staining was judged as positive staining for ALDH1.

Xenograft transplantation

Sorted cells were collected and re-suspended at concentrations of 10^2–10^4 cells per 50 μl of PBS and then mixed with 50 μl of matrigel (BD Biosciences). The cell-matrigel mixture was injected in the subcutaneous space of 6-week-old non-obese diabetic/severe combined immune-deficiency (NOD/SCID) mice (NOD.CB17-Prdkcscid/J, Charles River Laboratory, Yokohama, Japan) under anaesthesia. Tumor growth was monitored weekly, and tumor volume was calculated by $XY^2/2$ (X = long axis, Y = short axis).

Sphere formation assay

Spherical colony formation assay was performed using CSC Complete Recombinan Medium (Cell Systems Corporation, Kirkland, WA, USA). SP/$ALDH^{Br}$, SP/$ALDH^{Low}$, MP/$ALDH^{Br}$ and MP/$ALDH^{Low}$ cells were plated at 10^3 cells per well in 6-well ultra-low attachment plates (Corning Inc., Corning, NY, 14831) and cultured for 10 days. The morphology of the cells was assessed and pictures were taken under a light microscope every day. Round cell clusters larger than 100 μm were judged as spheres.

Cell viability assay

For cell viability assay, SP/$ALDH^{Br}$, SP/$ALDH^{Low}$, MP/$ALDH^{Br}$ and MP/$ALDH^{Low}$ cells were isolated. Then, the cells were plated at 1000 cells per 96-well plate for 1 day and then were treated with cisplatin for 3 days under several concentrations. Subsequently, the cell viability was investigated using the Premix WST-1 Cell Proliferation Assay System (Takara Bio Inc., Otsu, Japan) according to the manufacturer's protocol.

Adipocyte differentiation assay

For adipocyte differentiation assay, SP/$ALDH^{Br}$, SP/$ALDH^{Low}$, MP/$ALDH^{Br}$ and MP/$ALDH^{Low}$ cells were isolated. The cells were plated at 10000 cells per 24-well plate, and were grown in serum-reduced RPMI:DMEM (1:1) medium containing 0.5 mM trans-retinoic acid (Sigma-Aldrich) and 50 nM insulin (Sigma-Aldrich) for 2 days followed by the addition of adipose differentiation medium containing 170 nM insulin, 2 nM triiodothyronine and 0.5 mM rosiglitazone [19]. Cells were maintained in the medium for 5 days and neutral lipid accumulation was detected in 4% formaldehyde fixed cells using Oil red O (Sigma-Aldrich)

staining. Lipid staining was observed using microscope, and lipid stained cells were counted.

SOX2 mRNA knockdown by siRNA

A *SOX2* gene knockdown experiment was performed using small interfering RNA (siRNA). SOX2 siRNA (NM003106) and negative control siRNA were purchased from Life Technologies. MCAS cells were seeded into a 24-well plate, and transfections were carried out using Lipofectamine RNAi max (Life Technologies) in Opti-MEM according to the manufacturer's instructions. Fourty-eight hours later, the cells were analyzed for expression of *SOX2*, *ALDH1A1* and *ABCG2* by RT-PCR.

Reverse transcription polymerase chain reaction (RT-PCR) analysis

Gene knockdown of SOX2 was confirmed by RT-PCR. Isolation of RNA and RT-PCR analysis were performed as described previously [20]. The thermal cycling conditions were 94°C for 2 min, followed by 35 cycles of 15 sec at 94°C, 30 sec at 60°C, and 30 sec at 72°C. Primer pairs used for RT-PCR analysis were 5′-TGTTAGCTGATGCCGACTTG-3′ and 5′-TTCT-TAGCCCGCTCAACACT-3′ for *ALDH1A1* with an expected PCR product size of 154 base pairs (bps), 5′-CACCT-TATTGGCCTCAGGAA-3′ and 5′- CCTGCTTGGAAGGC-TCTATG-3′ for *ABCG2* with an expected PCR product size of 206 bps, 5′-CATGATGGAGACGGAGCTGA-3′ and 5′-AC-CCCGCTCGCCATGCTATT-3′ for *SOX2* with an expected PCR product size of 410 bps, 5′-GCAGTCAACAGTCGAA-GAAGG-3′, and 5′-ACCACAGTCCATGCCATCAC-3′ and 5′-TCCACCACCCTGTTGCTGTA-3′ for *glyceraldehyde-3-phosphate dehydrogenase (GAPDH)* with an expected product size of 452 bps. *GAPDH* was used as an internal control.

Quantitative real-time PCR analysis (qPCR)

Quantitative real-time PCR was performed using the ABI PRISM 7000 Sequence Detection System (Applied Biosystems, Foster City, CA) according to the manufacturer's protocol. *SOX2* (Hs01053049_s1), *ABCG2* (Hs00184979_m1), *CD44* (Hs01075861_m1), *PROM1* (Hs01009250_m1) and *ABCB1* (Hs00184500_m1) primers and probes were designed by the manufacturer (TaqMan Gene expression assays; Applied Biosystems). Thermal cycling was performed using 40 cycles of 95°C for 15 seconds followed by 60°C for 1 min. Each experiment was done in triplicate, and normalized to the *GAPDH* gene as an internal control.

Results

CSCs/CICs were enriched in SP cells

Ovarian CSCs/CICs have been isolated as SP cells from human and mice ovarian cancer line cells [11,21]. We analyzed several gynecological caner cell lines including human ovarian cell lines (MCAS, HTBoA, OVCAR3, OVSAHO) and human endometrial carcinoma (HEC-1) cell line (Figure 1A and Figure S1). SP cells could be detected in all line cells and the SP cell ratio were ranged from 1.2% to 2.6%. Since there is no report describing human mucinous adenocarcinoma line cell MCAS, we thus further analyzed SP cells derived from MCAS. CSCs/CICs have high tumor-initiating ability [22], we thus injected serially diluted numbers of SP cells and MP cells into the backs of three NOD/SCID mice subcutaneously to examine the tumor-initiating ability. In all three mice, tumors were initiated with 10^4 SP cells, and tumors were initiated with 10^4 MP cells in 2 of the 3 mice. In one mouse, a tumor was initiated with 10^3 SP cells, while 10^3 MP cells did not initiate any tumor (Table 1). The size of tumors derived from SP cells was significantly larger than that of tumors derived from MP cells (Figure 1B). The expression levels of stem cell markers were investigated by qPCR, and SP cells derived from MCAS cells expressed higher levels of the stem cell markers *SOX2*, *CD44* and *PROM1* and the ABC transporter gene *ABCG2*, whereas *ABCB1* was not (Figure 1C). These results indicate that CSCs/CICs were enriched in SP cells derived from MCAS cells. The results were reproduced in at least three independent experiments.

CSCs/CICs were enriched in ALDH^{Br} cells

CSCs/CICs could be isolated as ALDH^{Br} cells by the ALDEFLUOR assay [23]. We therefore examined whether CSCs/CICs can be successfully isolated by the ALDEFLUOR assay. MCAS, HTBoA, OVCAR3, OVSAHO and HEC-1 cells were analyzed by the ALDEFLUOR assay and we found that the ratio of ALDH^{Br} cells was 8.1% to 11.3% (Figure 2A and Figure S1). ALDH^{Br} cells and ALDH^{Low} cells derived from MCAS were sorted and injected into the backs of five NOD/SCID mice to examine the tumor-initiating ability. In all five mice, tumors were initiated with 10^4 ALDH^{Br} cells, while tumors were initiated with 10^4 ALDH^{Low} cells in only 2 of the 5 mice (Table 1). The size of tumors derived from ALDH^{Br} cells was significantly larger than that of tumors derived from ALDH^{Low} cells (Figure 2B). The expression levels of stem cell markers were investigated by qPCR. ALDH^{Br} cells derived from MCAS cells expressed higher levels of the stem cell markers *SOX2*, *CD44* and *PROM1*, ALDH1A1, and the ABC transporter gene *ABCG2* and *ABCB1* (Figure 1C). These results indicate that CSCs/CICs were also enriched in ALDH^{br} cell derived from MCAS cells. The results were reproduced in at least three independent experiments.

SP and ALDEFLUOR dual analysis

SP cells and ALDH^{Br} cells show greater efflux of Hoechst 33342 dye and higher expression level of aldehyde dehydrogenese, which are different phenotypes, and hematopoietic stem cells were isolated as an SP and ALDH^{Br} population in a previous study [24]. We therefore investigated the overlapping population of SP cells and ALDH^{Br} cells. After staining the MCAS cells with Hoechst 33342 dye, the cells were washed and then stained with ALDEFLUOR reagent and analyzed. In this experiment, the ratio of SP cells was 5.3% and the ratio of ALDH^{Br} cells was 14.4%. 7.1% of ALDH^{Br} cells showed SP population, and 6.9% of ALDH^{Mid} cells showed SP population, and only 3.7% of ALDH^{Low} cells showed SP population (Figure 3A). ALDH^{Br} cells exhibited partial overlapping, and only 1.0% of total cells (7.1% of 14.4% population) expressed both SP cell phenotype and ALDH^{Br} phenotype (Figure 3A).

SP and ALDH^{br} cells have high tumor-initiating ability

The tumor-initiating ability of SP and ALDH^{Br} (SP/ALDH^{Br}) cells was examined by injecting 10^3 and 10^2 cells, respectively, into NOD/SCID mice. Surprisingly, tumors were initiated with 10^3 SP/ALDH^{Br} cells and with as few as 10^2 SP/ALDH^{Br} cells in all mice (Table 1). Furthermore, tumors derived from SP/ALDH^{Br} cells showed significantly faster growth than that of tumors derived from SP cells and ALDH^{Br} cells (Figure 3B). These results indicate that SP/ALDH^{Br} cells are extremely enriched with CICs/CSCs.

We performed immunohistochemical staining to detect SP/ALDH^{Br} population in primary human ovarian carcinoma tissue. We used anti-ABCG2 antibody to detect SP cells, since SP cells are known to express higher level of ABCG2. As shown in figure 3C, dual positive (ABCG2-positive and ALDH1-positive)

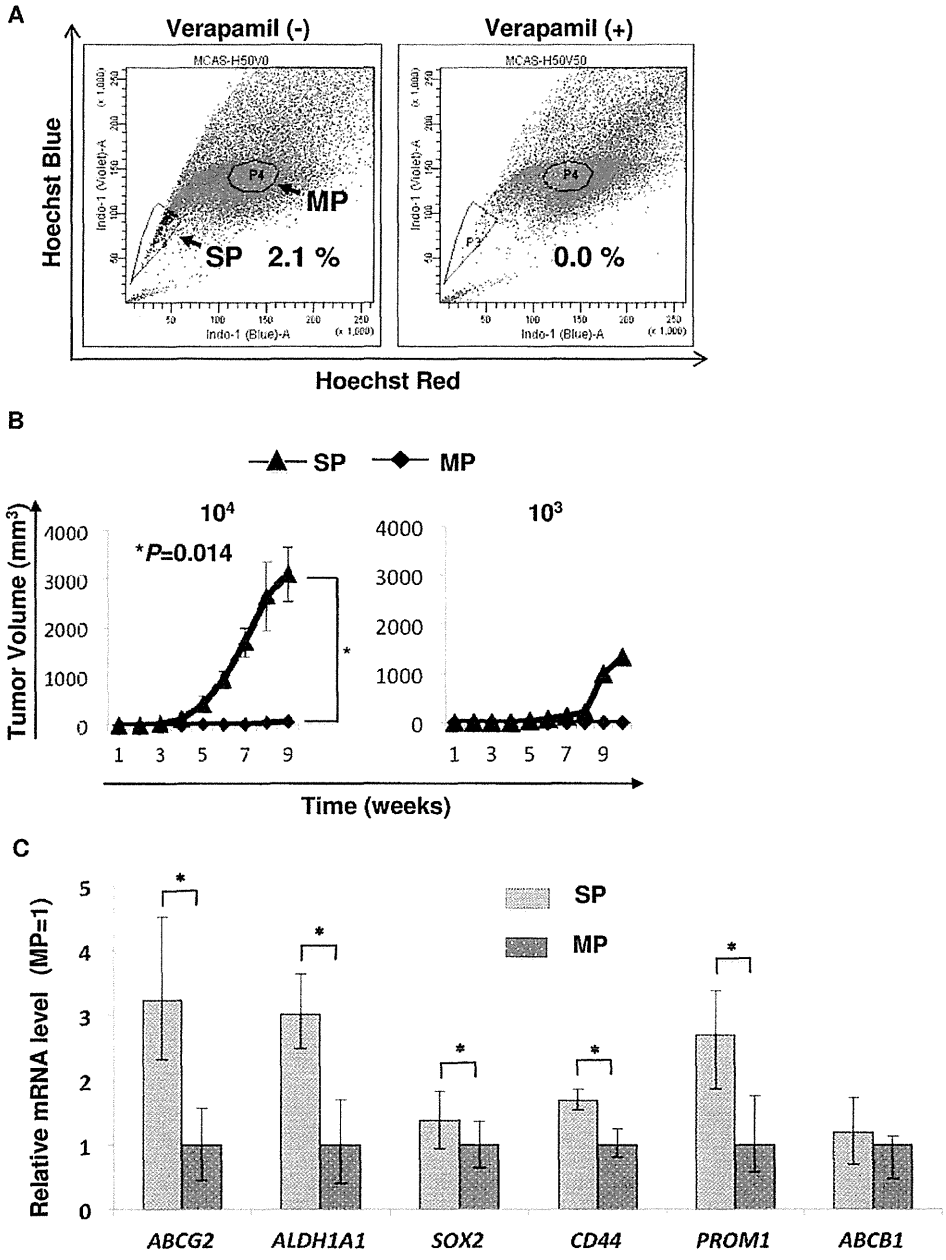

Figure 1. MCAS CSCs/CICs are enriched in SP cells. A. Detection of SP cells from MCAS cells. MCAS ovarian mucinous adenocarcinoma cells were stained with Hoechst 33342 dye and analyzed. The percentage represents the ratio of SP cells. B. Tumor initiation of SP cells derived from MCAS cells. 10^3 and 10^4 SP and MP cells derived from MCAS cells were inoculated subcutaneously into the backs of NOD/SCID mice, and tumor growth was measured weekly. Data represent means ± SD. Differences between SP and MP cells were examined for statistical significance using Student's t-test. *P values. C. qPCR of CSC/CIC markers in MCAS SP and MP cells. Data represent means ± SD. Asterisks indicate significant difference. *P<0.05. t-test.
doi:10.1371/journal.pone.0068187.g001

ovarian cancer cells were detectable in ovarian carcinoma tissue. Interestingly, some dual-positive cells exist next to vessels, might be indicating ovarian CSCs/CICs exist in vascular niche. SP/ALDH^{Br} cells were detected also from other ovarian serous adenocarcinoma line cells (OVSAHO, OVCAR3 and HTBoA) and an endometrial cell line (HEC-1), and the ratios of SP/ALDH^{Br} cells were 0.1% to 0.8% (Figure S1).

SP/ALDH^{Br} cells have stem cell phenotypes

The SP/ALDH^{Br} population was compared with other populations by the sphere forming assay. SP/ALDH^{Br}, SP/ALDH^{Low}, MP/ALDH^{Br} and MP/ALDH^{Low} cells were isolated from MCAS cells and cultured in an ultra-low attachment condition for the sphere forming assay. SP/ALDH^{Br} cells exhibited higher sphere formation efficiency than that of MP/

Table 1. Summary of tumor initiation incidence.

MCAS Cell	Tumor initiation (injected cell number)*		
	10^2	10^3	10^4
SP/ALDH^{Br} cells	5/5	5/5	n.d.
SP cells	0/3	1/3	3/3
ALDH^{Br} cells	0/5	0/5	5/5
MP cells	0/3	0/3	2/3
ALDH^{Low} cells	0/5	0/5	2/5
MP/ALDH^{Low} cells	0/5	0/5	0/5

*Tumor-initiating abilities were evaluated at day 70 post cell injection. Tumor-initiation/injection.
n.d.: not determined.
doi:10.1371/journal.pone.0068187.t001

ALDH^{Br} cells and MP/ALDH^{Low} cells (Figure 4A). The difference between SP/ALDH^{Br} cells and SP/ALDH^{Low} cells was not significant; however, SP/ALDH^{Br} cells tend to have higher sphere formation efficiency than that of SP/ALDH^{Low} cells.

CSCs/CICs have been described to have pluripotency [25], we thus analyzed the adipocyte differentiation ability of SP/ALDH^{Br} cells (Figure 4B). Isolated SP/ALDH^{Br}, SP/ALDH^{Low}, MPALDH^{Br} and MP/ALDH^{Low} population were cultured in an adypocyte differentiation condition. SP/ALDH^{Br} cells derived from MCAS cells revealed highest adipocyte differentiation ability compared with SP/ALDH^{Low}, MP/ALDH^{Br} and MP/ALDH^{Low} cells derived from MCAS cells.

CSCs/CICs are resistant to chemotherapy [4], we thus analyzed drug resistance of SP/ALDH^{Br} cells. Since cisplatin is a key drug for ovarian carcinoma chemotherapy, we used cisplatin. Isolated SP/ALDH^{Br}, SP/ALDH^{Low}, MPALDH^{Br} and MP/ALDH^{Low} population were cultured in an existence of cisplatin. SP/ALDH^{Br} cells significantly higher cisplatin resistance compared with SP/ALDH^{Low} cells, MP/ALDH^{Br} cells and MP/ALDH^{Low} cells. And, MP/ALDH^{Low} cells exhibited highest sensitivity to cisplatin (Figure 5A).

To analyze the molecular characteristics of SP/ALDH^{Br} population, we performed qPCR (Figure 5B). *ABCG2* mRNA was preferentially expressed in SP/ALDH^{Br} cells and SP/ALDH^{Low} cells. *ALDH1A1* was expressed in SP/ALDH^{Br} cells and MP/ALDH^{Br} cells. These expression profiles are consistent with the fact that the SP cell phenotype depends on the expression of *ABCG2* and the ALDH^{Br} cell phenotype depends on the expression of *ALDH1A1*. *SOX2* mRNA was expressed at highest level in SP/ALDH^{Br} cells but not in SP/ALDH^{Low} cells, MP/ALDH^{Br} cells or MP/ALDH^{Low} cells (Figure 5B), indicating that the SP/ALDH^{Br} population preferentially include a stem cell population. Since SOX2 has a role in the maintenance of lung CSCs/CICs [26], we investigated the relation of *SOX2* and expressions of *ABCG2* and *ALDH1A1*. The expressions of *ABCG2* and *ALDH1A1* were reduced in *SOX2* mRNA knocked down cells (Figure 5C). Furthermore, SOX2 knocked down cells showed lower tumor-initiation than that of control siRNA transfected MCAS cells (Figure 5D). Therefore, these results suggest that SP/ALDH^{Br} population express high level of stem cell gene *SOX2*, which may have role in the maintenance of CSCs/CICs and expressions of *ABCG2* and *ALDH1A1*.

The expression levels of CD44, a representative marker for ovarian CSCs/CICs [27,28], was similar in all populations (Figure 5B). We therefore investigated the relation of SP cells, ALDH^{Br} cells and CD44-positive (CD44$^+$) cells. The ratio of CD44$^+$ cells was 8.0%. The ratio of SP/CD44$^+$ overlapping population was 0.9%, and the ratio of ALDH^{Br}/CD44$^+$ overlapping population was 3.3%. Furthermore, the ratio of SP/ALDH^{Br}/CD44$^+$ overlapping population was 0.4% (Figure 6).

Discussion

The concept of CSCs/CICs was proposed long time ago [29]. Leukemia stem cells have been isolated from acute leukemic cells [30,31], and the first CSC/CIC population was isolated from breast carcinoma with the combination of CD44 and CD24 expression [32]. In the following works, CSCs/CICs were successfully isolated in several malignancies. However, since the molecular mechanisms of CSCs/CICs are still elusive, accurate markers for CSCs/CICs are still unknown. Therefore, improvements in methods for isolation of CSCs/CICs are still needed.

Combination methods with double or triple markers and with markers and ALDEFLUOR assay have been reported. The populations of ALDH^{Br} and CD44$^+$/CD24$^-$ cells exhibited partial overlapping, and the ALDH^{Br}/CD44$^+$/CD24$^-$ population showed higher tumor-initiating ability than that of the ALDH^{Br} population or CD44$^+$/CD24$^-$ population [17]. The ALDH^{Br}/CD44$^+$ population and ALDH^{Br}/CD133$^+$ population derived from human primary colon carcinoma exhibited higher tumor-initiating ability than that of ALDH^{Br}, CD44$^+$ and CD133$^+$ populations [33]. These findings indicate that the expressions of CSC/CIC markers are partially overlapped and that the overlapped population is highly enriched with CSCs/CICs. Indeed, our results also showed similar overlapping of ALDH^{Br} cells and SP cells, and the overlapping population exhibited higher tumor-initiating ability. In an ovarian cancer study, ALDH^{Br} cells were more enriched in CD44$^+$ cells than in use of the CD133$^+$ cells [23], but the ALDH^{Br} and CD44$^+$ overlapping was partial. We identified SP/ALDH^{Br}/CD44$^+$ overlapping population from MCAS cells (Figure 6). Therefore, use of the overlapping population of SP/ALDH^{Br}/CD44$^+$ cells may be a better approach to identify CSC/CIC populations.

Glioma stem cells have been described to differentiate into endothelial cells [34]. Malignant methotelioma stem cells have been described to differentiate into endothelial cells, neural cells and adipocytes [25]. In this study, we confirmed that SP/ALDH^{Br} cells have higher adipocyte differentiation ability. Therefore, ovarian cancer stem cells might have potential to differentiate into different lineage cells, suggesting that ovarian cancer stem cells are immature state. SOX2, a key factor for cell reprogramming [35], was expressed in SP/ALDH^{Br} cells at highest level. And knockdown of SOX2 reduced the expressions of *ABCG2* and *ALDH1A1*. Thus SOX2 might have a role to sustain immature state of ovarian cancer stem cells.

CSCs/CICs are described to be resistant to chemotherapy [4]. Indeed SP/ALDH^{Br} cells showed higher cisplatin resistance than did SP/ALDH^{Low} cells, MP/ALDH^{Br} cells and MP/ALDH^{Low} cells. Several mechanisms of drug resistance have been described, such as CSCs/CICs are dormant state, CSCs/CICs express higher levels of transporters, CSCs/CICs express higher levels of inhibitor of apoptosis proteins (IAPs) and so on. In this study, only SP/ALDH^{Br} population expressed both *ABCB1* and *ABCG2* transporters among SP/ALDH^{Br}, SP/ALDH^{Low}, MP/ALDH^{Br} and MP/ALDH^{Low} cells (Figure 6B). Thus, higher expressions of transporters might be one mechanisms of drug resistance of SP/ALDH^{Br} cells.

Dual SP and ALDH^{Br} cells in hematologic stem cells have been reported [24]. The overlapping population of ALDH^{Br} cells and CD133$^+$ cells has prominent tumorigenicity [36]. However, SP/

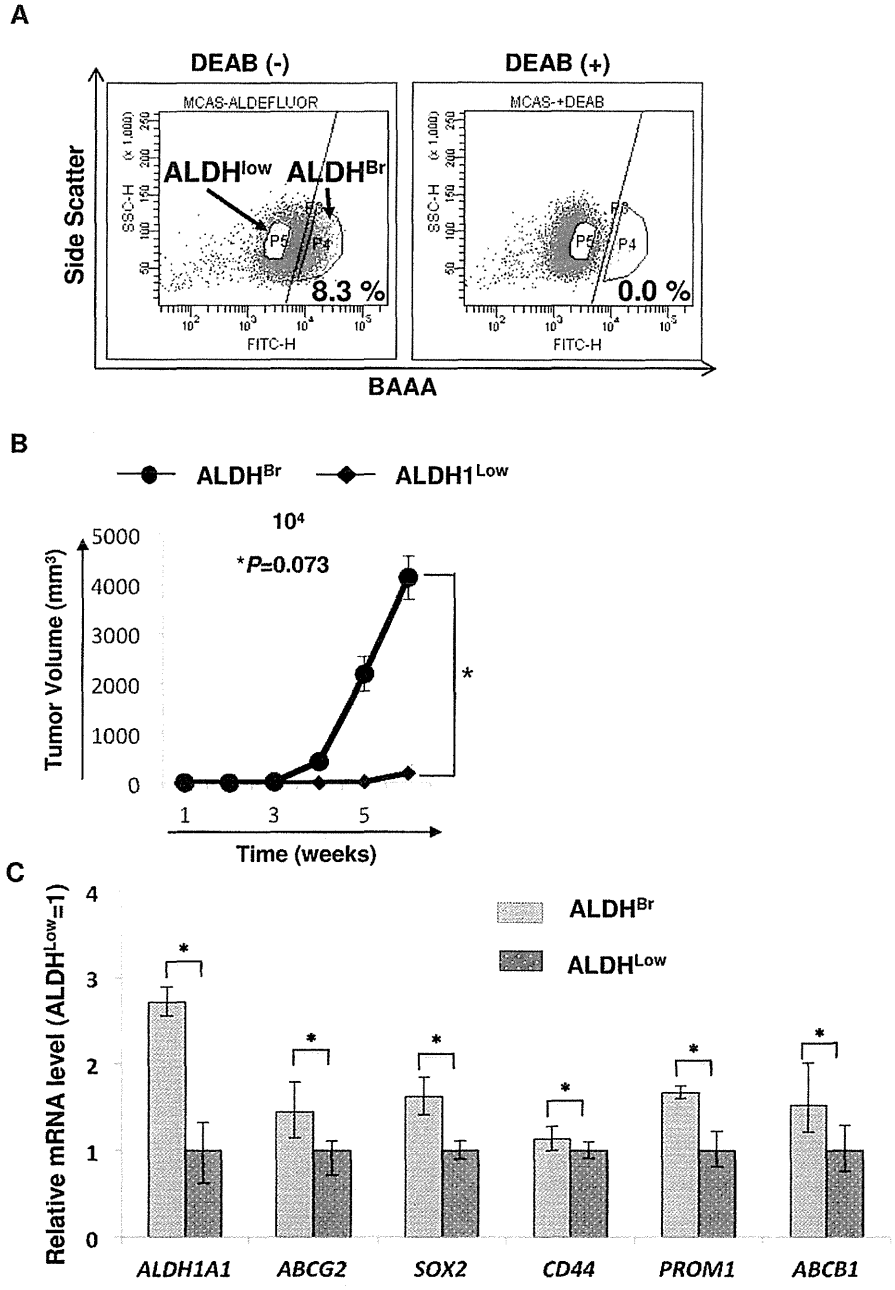

Figure 2. MCAS CSCs/CICs are enriched in ALDH^{Br} cells. A. Detection of ALDH^{Br} cells from MCAS cells. MCAS ovarian mucinous adenocarcinoma cells were stained with BAAA and analyzed. The percentage represents the ratio of ALDH^{Br} cells. Inhibitor indicate ALDH1 inhibitor (diethylamino- benzaldehyde (DEAB)). B. Tumor initiation of ALDH^{Br} cells derived from MCAS cells. 10^4 ALDH^{Br} and ALDH^{Low} cells derived from MCAS cells were inoculated subcutaneously into the backs of NOD/SCID mice, and tumor growth was measured weekly. Data represent means ± SD. Differences between ALDH^{Br} and ALDH^{Low} cells were examined for statistical significance using Student's t-test. *P values. C. qPCR of CSC/CIC markers in MCAS SP and MP cells. Data represent means ± SD. Asterisks indicate significant difference. *P<0.05. t-test.
doi:10.1371/journal.pone.0068187.g002

ALDH^{Br} cells have not been reported in solid tumors yet. SP cell phenotype represents the efflux of Hoechst 33342 dye due to the expression of ABC transporter, ABCG2, which may be involved in drug resistance [37]. ALDH^{Br} cells represent the higher expression of ALDH1, which may be involved in detoxification [38]. SP cells and ALDH^{Br} cells thus have different molecular properties, and the overlapping of SP cells and ALDH^{Br} cells were partial. And we found SP and ALDH^{Br} overlapping population was the highest CSCs/CICs enriched population which exhibited higher sphere formation, higher tumor-initiation, higher adipocyte differentia-

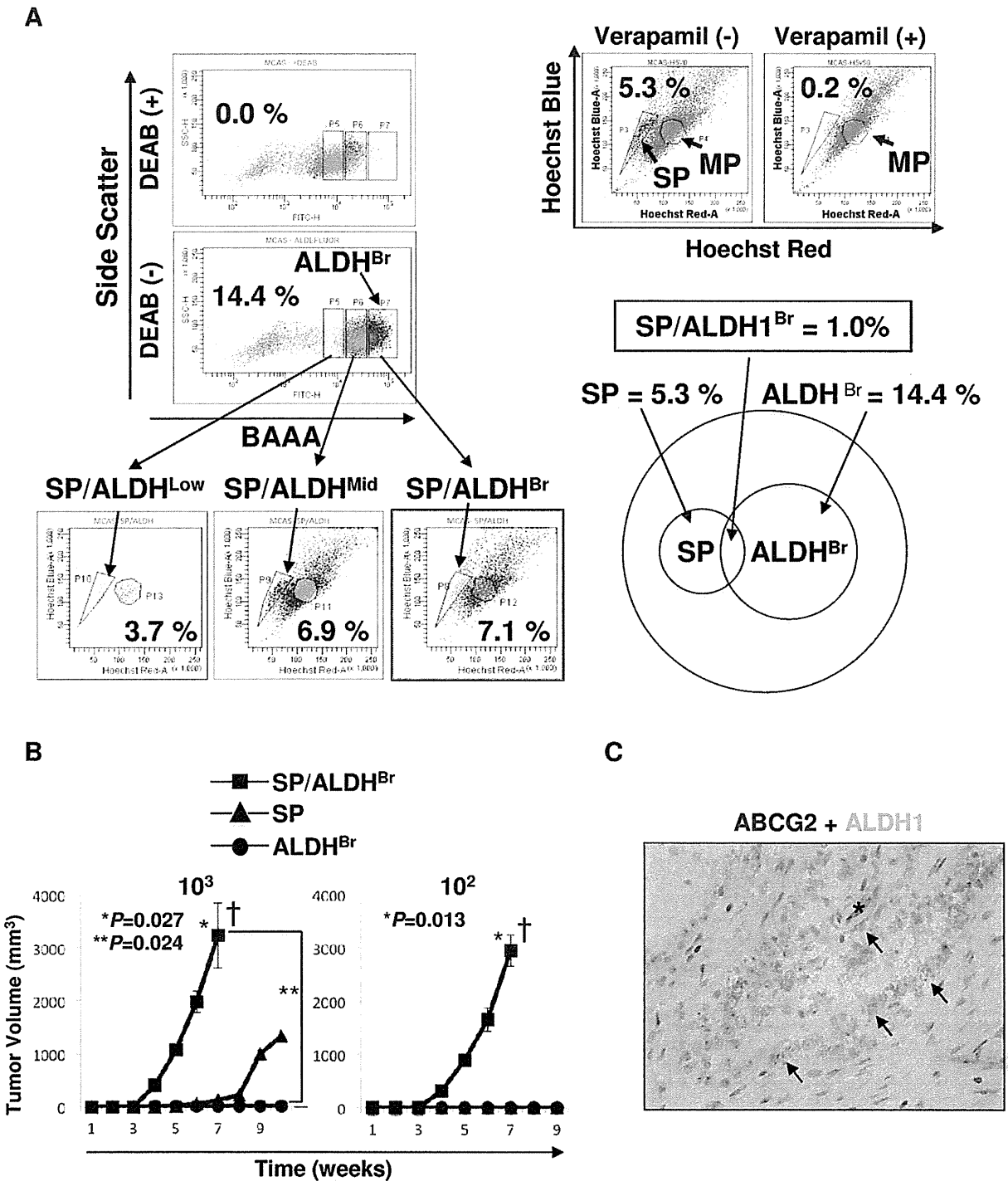

Figure 3. SP and ALDEFLUOR dual assay. A. Summary of SP and ALDEFLUOR dual assay. MCAS cells were stained by Hoechst 33342 dye and then stained by BAAA and analyzed. The cells were divided into three groups according to ALDH intensity ($ALDH^{Br}$ (ALDH bright), $ALDH^{Mid}$ (ALDH middle), $ALDH^{Low}$ (ALDH low)), then analyzed by SP assay. The ratio of $ALDH^{Br}$ cells was 14.4%, and the ratio of SP cells was 5.3%. The ratios of SP cells in $ALDH^{Br}$ cells, $ALDH^{Mid}$ cells and $ALDH^{Low}$ cells were 7.1%, 6.9% and 3.7%, respectively. The ratio of $SP/ALDH^{Br}$ cells in total cells was 1.0%. B. Tumor initiation of $SP/ALDH^{Br}$, SP and $ALDH^{Br}$ cells. 10^2 and 10^3 $SP/ALDH^{Br}$, SP and $ALDH^{Br}$ cells derived from MCAS cells were inoculated subcutaneously into the backs of NOD/SCID mice, and tumor growth was measured weekly. Data represent means ± SD. Differences between $SP/ALDH^{Br}$ and SP cells or $ALDH^{Br}$ cells were examined for statistical significance using Student's t-test. *P values. Daggers indicate mice death due to tumor. C. Immunohistochemical staining of ABCG2 and ALDH1. Ovarian carcinoma tissue was stained by anti-ABCG2 antibody and anti-ALDH1 antibody. Brown membrane staining indicates ABCG2 and cytoplasm pink staining indicates ALDH1. Asterisk indicates vessel, and arrows indicate ABCG2 and ALDH1 double-positive ovarian carcinoma cells. Magnification, ×400.
doi:10.1371/journal.pone.0068187.g003

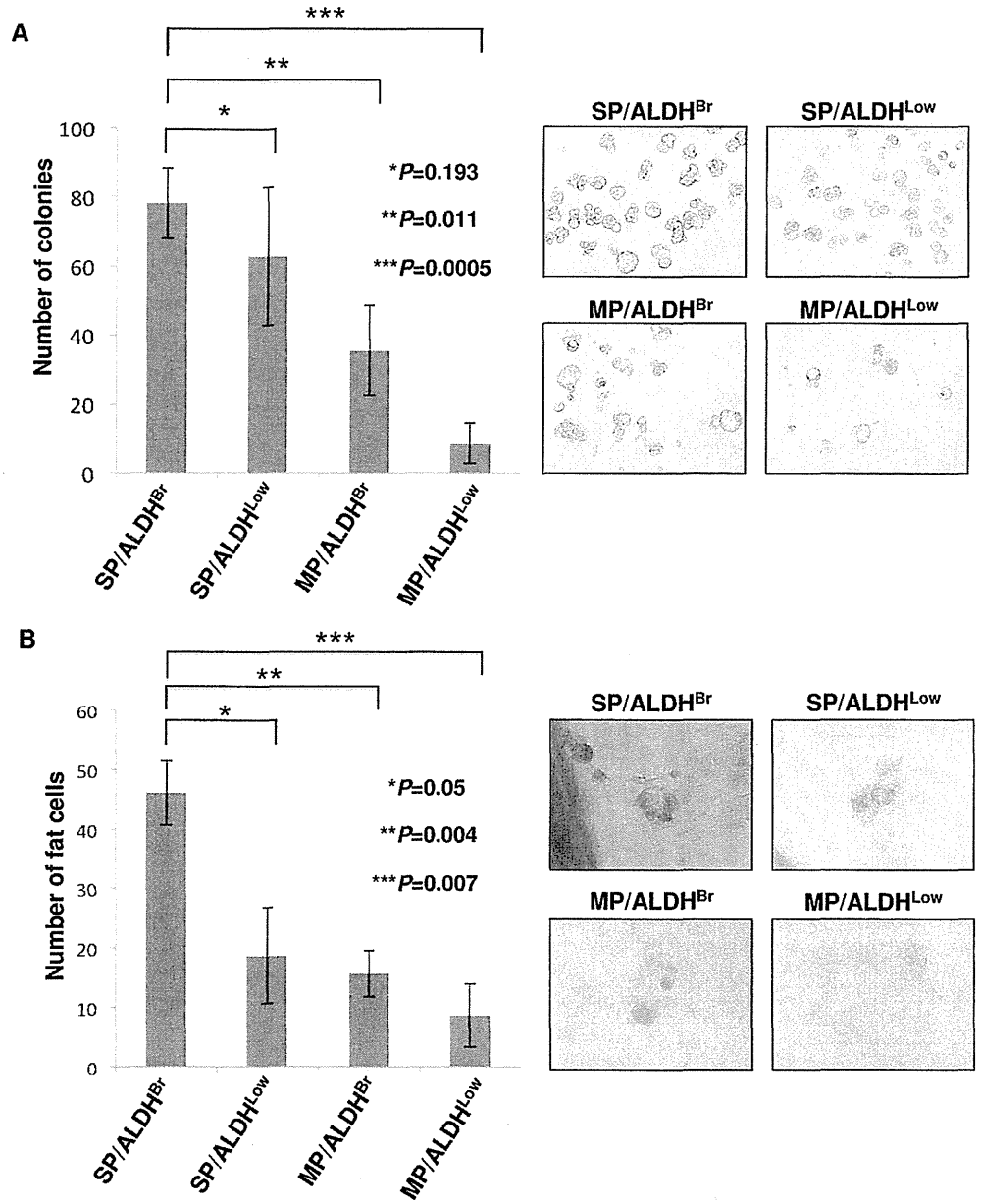

Figure 4. Characterization of SP/ADLH^{Br} cells. A. Sphere formation assay. The numbers of colonies from four fractions (SP/ALDH^{Br}, SP/ALDH^{Low}, MP/ALDH^{Br} and MP/ALDH^{Low}) were evaluated at day 7. Data represent means ± SD. The differences were examined for statistical significance using Student's t-test. *P values. Representative images of spheres are shown (×100). B. Adipocyte differentiation assay. The cells were cultured under existence of trans-retinoic acid followed by adipocyte differentiation medium. Oli Red O-positive adipocytes were counted. Data represent means ± SD. The differences were examined for statistical significance using Student's t-test. *P values. Representative images of Oil Red O-staining are shown (×200). Red-staining indicate adipocyte differentiation.
doi:10.1371/journal.pone.0068187.g004

tion ability, higher drug resistance and higher expression level of SOX2, a representative marker of CSCs/CICs, which is related to the tumor-initiating ability of CSCs/CICs [26]. Therefore, SP/ALDH^{Br} population is the better source of CSCs/CICs than SP cells or ALDH^{Br} cells that have been previously described. We found that SOX2 is expressed at high level in SP/ALDHBr cells, and knockdown of SOX2 suppressed the expressions of *ALDH1A1* and *ABCG2*, and suppressed tumor-initiation. Thus, SOX2 might has role in the maintenance of both SP cell and ALDH^{Br} cell population, and also has role in the maintenance of ovary CSCs/CICs.

In summary, SP/ALDH^{Br} cells comprise a more highly CSC/CIC- enriched popuration than do SP cells or ALDH^{Br} cells, and further analysis of SP/ALDH^{Br} cells should lead to elucidation of the molecular mechanisms of CSCs/CICs.

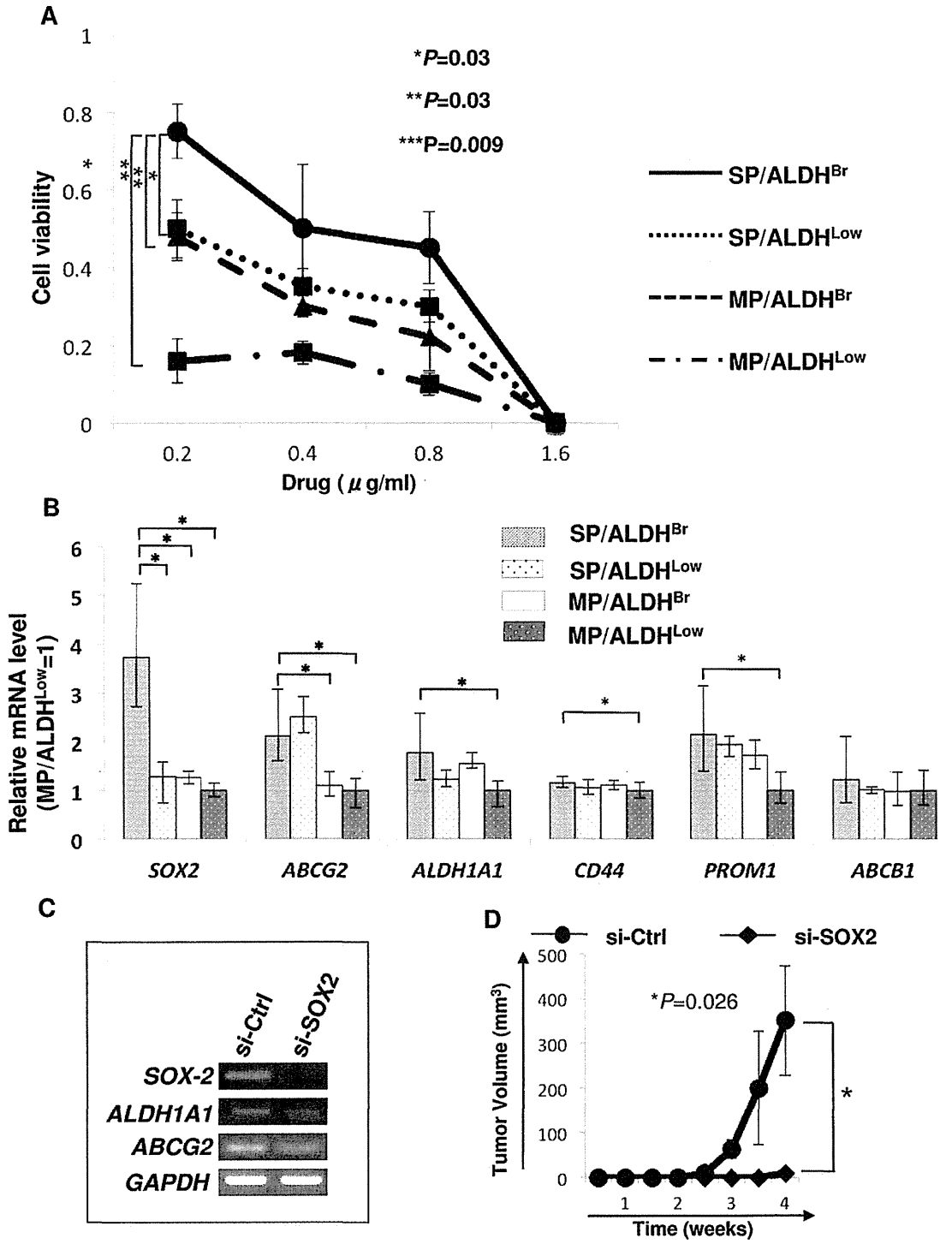

Figure 5. Charasterization of SP/ALDHBr cells. A. Cell viability assay. The cells were cultured under existence of serially diluted cisplatin. The viable cells were analyzed by WST-1 kit. Y-axis indicates the viability of cells. Data represent means ± SD. The differences were examined for statistical significance using Student's t-test. *P values. B. qPCR analysis. The expression of stem cell markers was examined using SP/ALDH^{Br}, SP/ALDH^{Low}, MP/ALDH^{Br} and MP/ALDH^{Low} cells. Data represent means ± SD. Asterisks indicate significant difference. *P<0.05. t-test. C. *SOX2* knockdown suppress the expressions of *ALDH1A1* and *ABCG2*. *SOX2* mRNA was knocked down by siRNA. Two days after transfection of SOX2 siRNA, the expressions of *ALDH1A1* and *ABCG2* were investigated by RT-PCR. *GAPDH* was used as an internal control. Control siRNA (si-Cont) transfected cells were used as negative control. D. SOX2 knock down suppress the tumor-initiation. *SOX2* mRNA was knocked down by siRNA. Ten thousand si-SOX2 and control siRNA (si-Cont) transfected cells were inoculated subcutaneously into the backs of NOD/SCID mice, and tumor growth was measured weekly. Data represent means ± SD. Differences were examined for statistical significance using Student's t-test. *P values.
doi:10.1371/journal.pone.0068187.g005